1. Harris, E.D. 1997. *Rheumatoid arthritis.* W.B. Saunders. Philadelphia, Pennsylvania, USA. 417 pp.
2. Feldmann, M., Brennan, F.M., and Maini, R.N. 1996. Role of cytokines in rheumatoid arthritis. *Annu. Rev. Immunol.* **14**:397–440.
3. Choy, E.H., et al. 2002. Therapeutic benefit of blocking interleukin-6 activity with an anti-interleukin-6 receptor monoclonal antibody in rheumatoid arthritis: a randomized, double-blind, placebo-controlled, dose-escalation trial. *Arthritis Rheum.* **46**:3143–3150.
4. Elliott, M.J., et al. 1993. Treatment of rheumatoid arthritis with chimeric monoclonal antibodies to tumor necrosis factor alpha. *Arthritis Rheum.* **36**:1681–1690.
5. van de Loo, F.A., Kuiper, S., van Enckevort, F.H., Arntz, O.J., and van den Berg, W.B. 1997. Interleukin-6 reduces cartilage destruction during experimental arthritis. A study in interleukin-6-deficient mice. *Am. J. Pathol.* **151**:177–191.
6. Sasai, M., et al. 1999. Delayed onset and reduced severity of collagen-induced arthritis in interleukin-6-deficient mice. *Arthritis Rheum.* **42**:1635–1643.
7. Anguita, J., et al. 1998. Borrelia burgdorferi-infected, interleukin-6-deficient mice have decreased Th2 responses and increased lyme arthritis. *J. Infect. Dis.* **178**:1512–1515.
8. Alonzi, T., et al. 1998. Interleukin 6 is required for the development of collagen-induced arthritis. *J. Exp. Med.* **187**:461–468.
9. Ji, H., et al. 2002. Critical roles for interleukin 1 and tumor necrosis factor alpha in antibody-induced arthritis. *J. Exp. Med.* **196**:77–85.
10. Joosten, L.A., Helsen, M.M., van de Loo, F.A., and van den Berg, W.B. 1996. Anticytokine treatment of established type II collagen-induced arthritis in DBA/1 mice. A comparative study using anti-TNF alpha, anti-IL-1 alpha/beta, and IL-1Ra. *Arthritis Rheum.* **39**:797–809.
11. Takayanagi, H., et al. 2000. T-cell-mediated regulation of osteoclastogenesis by signalling cross-talk between RANKL and IFN-gamma. *Nature.* **408**:600–605.
12. Sakaguchi, N., et al. 2003. Altered thymic T-cell selection due to a mutation of the ZAP-70 gene causes autoimmune arthritis in mice. *Nature.* **426**:454–460.
13. Firestein, G.S., Yeo, M., and Zvaifler, N.J. 1995. Apoptosis in rheumatoid arthritis synovium. *J. Clin. Invest.* **96**:1631–1638.
14. van Dinther-Janssen, A.C., et al. 1991. The VLA-4/VCAM-1 pathway is involved in lymphocyte adhesion to endothelium in rheumatoid synovium. *J. Immunol.* **147**:4207–4210.
15. Kuhn, R., Lohler, J., Rennick, D., Rajewsky, K., and Muller, W. 1993. Interleukin-10-deficient mice develop chronic enterocolitis. *Cell.* **75**:263–274.
16. Arend, W.P. 2001. Physiology of cytokine pathways in rheumatoid arthritis. *Arthritis Care Res.* **45**:101–106.
17. Probert, L., Plows, D., Kontogeorgos, G., and Kollias, G. 1995. The type I interleukin-1 receptor acts in series with tumor necrosis factor (TNF) to induce arthritis in TNF-transgenic mice. *Eur. J. Immunol.* **25**:1794–1797.
18. Dayer, J.M., Beutler, B., and Cerami, A. 1985. Cachectin/tumor necrosis factor stimulates collagenase and prostaglandin E2 production by human synovial cells and dermal fibroblasts. *J. Exp. Med.* **162**:2163–2168.
19. Miyasaka, N., et al. 1988. Augmented interleukin-1 production and HLA-DR expression in the synovium of rheumatoid arthritis patients. Possible involvement in joint destruction. *Arthritis Rheum.* **31**:480–486.
20. Guerne, P.A., Zuraw, B.L., Vaughan, J.H., Carson, D.A., and Lotz, M. 1989. Synovium as a source of interleukin 6 in vitro. Contribution to local and systemic manifestations of arthritis. *J. Clin. Invest.* **83**:585–592.
21. Charles, P., et al. 1999. Regulation of cytokines, cytokine inhibitors, and acute-phase proteins following anti-TNF-alpha therapy in rheumatoid arthritis. *J. Immunol.* **163**:1521–1528.
22. Kishimoto, T., Taga, T., and Akira, A. 1994. Cytokine signal transduction. *Cell.***76**:253–262.
23. Lockslay, R.M., Killeen, N., and Leonardo, M.J. 2001. The TNF and TNF receptor superfamilies: integrating mammalian biology. *Cell.* **104**:487–501.
24. Firestein, G.S., and Manning, A.M. 1999. Signal transduction and transcription factors in rheumatic diseases. *Arthritis Rheum.* **42**:609–621.
25. Chu, C.Q., Field, M., Feldmann, M., and Maini, R.N. 1991. Localization of tumor necrosis factor alpha in synovial tissues and at the cartilage-pannus junction in patients with rheumatoid arthritis. *Arthritis Rheum.* **34**:1125–1132.
26. Ulfgren, A.K., Lindblad, S., Klareskog, L., Anderson, J., and Anderson, U. 1995. Detection of cytokine producing cells in the synovial membrane from patients with rheumatoid arthritis. *Ann. Rheum. Dis.* **54**:654–661.
27. Marinova-Mutafchieva, L., et al. 1997. Dynamics of proinflammatory cytokine expression in the joints of mice with collagen-induced arthritis (CIA). *Clin. Exp. Immunol.* **107**:507–512.
28. Okada, Y., Takeuchi, N., Tomita, K., Nakanishi, I., and Nagase, H. 1989. Immunolocalization of matrix metalloproteinase 3 (stromelysin) in rheumatoid synovioblasts (B cells): correlation with rheumatoid arthritis. *Ann. Rheum. Dis.* **48**:645–653.
29. Tanaka, J., et al. 2000. Lipopolysaccharide-induced HIV-1 expression in transgenic mice is mediated by tumor necrosis factor-alpha and interleukin-1, but not by interferon-gamma nor interleukin-6. *AIDS.* **14**:1299–1307.
30. Feldmann, M., and Maini, R.N. 2001. Anti-TNF alpha therapy of rheumatoid arthritis: what have we learned? *Annu. Rev. Immunol.* **19**:163–196.
31. Persson, S., Mikulowska, A., Narula, S., O'Garra, A., and Holmdahl, R. 1996. Interleukin-10 suppresses the development of collagen type II-induced arthritis and ameliorates sustained arthritis in rats. *Scand. J. Immunol.* **44**:607–614.
32. Walmsley, M., et al. 1996. Interleukin-10 inhibition of the progression of established collagen-induced arthritis. *Arthritis Rheum.* **39**:495–503.
33. Katsikis, P.D., Chu, C.Q., Brennan, F.M., Maini, R.N., and Feldmann, M. 1994. Immunoregulatory role of interleukin 10 in rheumatoid arthritis. *J. Exp. Med.* **179**:1517–1527.
34. Asseman, C., Mauze, S., Leach, M.W., Coffman, R.L., and Powrie, F. 1999. An essential role for interleukin 10 in the function of regulatory T cells that inhibit intestinal inflammation. *J. Exp. Med.* **190**:995–1004.
35. Goudy, K.S., et al. 2003. Systemic overexpression of IL-10 induces $CD4^+CD25^+$ cell populations in vivo and ameliorates type 1 diabetes in nonobese diabetic mice in a dose-dependent fashion. *J. Immunol.* **171**:2270–2278.
36. Naka, T., Nishimoto, N., and Kishimoto, T. 2002. The paradigm of IL-6: from basic science to medicine [review]. *Arthritis Res.* **4**(Suppl. 3):S233–S242.
37. Pasare, C., and Medzhitov, R. 2003. Toll pathway-dependent blockade of $CD4^+CD25^+$ T cell-mediated suppression by dendritic cells. *Science.* **299**:1033–1036.
38. Morgan, M.E., et al. 2003. $CD25^+$ cell depletion hastens the onset of severe disease in collagen-induced arthritis. *Arthritis Rheum.* **48**:1452–1460.
39. Wu, A.J., Hua, H., Munson, S.H., and McDevitt, H.O. 2002. Tumor necrosis factor-alpha regulation of $CD4^+CD25^+$ T cell levels in NOD mice. *Proc. Natl. Acad. Sci. U. S. A.* **99**:12287–12292.
40. Ortmann, R.A., and Shevach, E.M. 2001. Susceptibility to collagen-induced arthritis: cytokine-mediated regulation. *Clin. Immunol.* **98**:109–118.
41. Joosten, L.A., et al. 1997. Role of interleukin-4 and interleukin-10 in murine collagen-induced arthritis. Protective effect of interleukin-4 and interleukin-10 treatment on cartilage destruction. *Arthritis Rheum.* **40**:249–260.
42. Dayer, J.M., and Burger, D. 1999. Cytokines and direct cell contact in synovitis: relevance to therapeutic intervention. *Arthritis Res.* **1**:17–20.
43. Miossec, P. 2003. Interleukin-17 in rheumatoid arthritis: if T cells were to contribute to inflammation and destruction through synergy. *Arthritis Rheum.* **48**:594–601.
44. Roosnek, E., and Lanzavecchia, A. 1991. Efficient and selective presentation of antigen-antibody complexes by rheumatoid factor B cells. *J. Exp. Med.* **173**:487–489.
45. Mageed, R.A., Borretzen, M., Moyes, S.P., Thompson, K.M., and Natvig, J.B. 1997. Rheumatoid factor autoantibodies in health and disease. *Ann. N. Y. Acad. Sci.* **815**:296–311.
46. Dalton, D.K., et al. 1993. Multiple defects of immune cell function in mice with disrupted interferon-gamma genes. *Science.* **259**:1739–1745.
47. Noben-Trauth, N., Kohler, G., Burki, K., and Ledermann, B. 1996. Efficient targeting of the IL-4 gene in a BALB/c embryonic stem cell line. *Transgenic Res.* **5**:487–491.
48. Hori, S., Nomura, T., and Sakaguchi, S. 2003. Control of regulatory T cell development by the transcription factor Foxp3. *Science.* **299**:1057–1061.
49. Sakaguchi, S., and Sakaguchi, N. 1990. Thymus and autoimmunity: Capacity of the normal thymus to produce pathogenic self-reactive T cells and conditions required for their induction of autoimmune disease. *J. Exp. Med.* **172**:537–545.

ARTHRITIS & RHEUMATISM
Vol. 50, No. 3, March 2004, pp 794–804
DOI 10.1002/art.20206

The Antirheumatic Drug Leflunomide Inhibits Osteoclastogenesis by Interfering With Receptor Activator of NF-κB Ligand–Stimulated Induction of Nuclear Factor of Activated T Cells c1

Makoto Urushibara,[1] Hiroshi Takayanagi,[2] Takako Koga,[2] Sunhwa Kim,[3] Miho Isobe,[2] Yasuyuki Morishita,[3] Takumi Nakagawa,[4] Monika Löeffler,[5] Tatsuhiko Kodama,[6] Hisashi Kurosawa,[4] and Tadatsugu Taniguchi[3]

Objective. **Suppression of bone destruction is required as part of an effective therapeutic strategy for autoimmune arthritis. Although numerous antirheumatic drugs are in clinical use, little is known about whether they inhibit bone destruction by acting on activated T cells or other cell types, such as bone-resorbing osteoclasts. This study was undertaken to determine whether leflunomide has a direct action on the osteoclast lineage and to gain insights into the molecular basis for the bone-protective effect of leflunomide.**

Methods. **The direct effect of leflunomide on osteoclast differentiation was investigated using an in vitro culture system of bone marrow monocyte/macrophages stimulated with receptor activator of NF-κB ligand (RANKL) and macrophage colony-stimulating factor. The molecular mechanism of the inhibition was analyzed by genome-wide screening. The T cell–independent effect of leflunomide was examined in *rag-2*$^{-/-}$ mice.**

Results. **Leflunomide blocked de novo pyrimidine synthesis and RANKL-induced calcium signaling in osteoclast precursor cells in vitro; hence, the induction of nuclear factor of activated T cells c1 (NF-ATc1) was strongly inhibited. The inhibition of this pathway is central to the action of leflunomide, since the inhibition was overcome by ectopic expression of NF-ATc1 in the precursor cells. Leflunomide suppressed endotoxin-induced inflammatory bone destruction even in *rag-2*$^{-/-}$ mice.**

Conclusion. **Leflunomide has a direct inhibitory effect on RANKL-mediated osteoclast differentiation by inhibiting the induction of NF-ATc1, the master switch regulator for osteoclast differentiation. Our study suggests that the direct inhibitory action of leflunomide on osteoclast differentiation constitutes an important aspect in the amelioration of bone destruction, and that the RANKL-dependent NF-ATc1 induction pathway is a promising target for pharmacologic intervention in arthritic bone destruction.**

Rheumatoid arthritis (RA) is an autoimmune disease characterized by chronic inflammation of syno-

Supported in part by a grant for Advanced Research on Cancer from the Ministry of Education, Culture, Sports, Science, and Technology of Japan, a grant from PRESTO, Japan Science and Technology Corporation (JST), a grant from the Center of Excellence (COE) Program for Frontier Research on Molecular Destruction and Reconstruction of Tooth and Bone, Grants-in-Aid for Scientific Research from the Ministry of Education, Culture, Sports, Science, and Technology of Japan and the Japan Society for the Promotion of Science, Health Sciences Research Grants from the Ministry of Health, Labour and Welfare of Japan, and a grant from the Japan Orthopaedics and Traumatology Foundation.

[1]Makoto Urushibara, MD: Graduate School of Medicine, University of Tokyo, Tokyo, Japan, and Juntendo University School of Medicine, Tokyo, Japan; [2]Hiroshi Takayanagi, MD, PhD, Takako Koga, MSc, Miho Isobe, BSc: Graduate School of Medicine, University of Tokyo, Tokyo, Japan, PRESTO, Japan Science and Technology Corporation, Saitama, Japan, and Graduate School, Tokyo Medical and Dental University and COE Program, Tokyo, Japan; [3]Sunhwa Kim, MSc, Yasuyuki Morishita, BSc, Tadatsugu Taniguchi, PhD: Graduate School of Medicine, University of Tokyo, Tokyo, Japan; [4]Takumi Nakagawa, MD, PhD, Hisashi Kurosawa, MD, PhD: Juntendo University School of Medicine, Tokyo, Japan; [5]Monika Löeffler, PhD: Molecular Enzymology Group, Institute for Physiological Chemistry, Philipps-University, Marburg, Germany; [6]Tatsuhiko Kodama, MD, PhD: Research Center for Advanced Science and Technology, University of Tokyo, Tokyo, Japan.

Drs. Urushibara and Takayanagi contributed equally to this work.

Address correspondence and reprint requests to Tadatsugu Taniguchi, PhD, Department of Immunology, Graduate School of Medicine and Faculty of Medicine, University of Tokyo, Hongo 7-3-1, Bunkyo-ku, Tokyo 113-0033, Japan. E-mail: tada@m.u-tokyo.ac.jp.

Submitted for publication June 4, 2003; accepted in revised form November 20, 2003.

vial joints, resulting in crippling bone destruction (1). Combined use of disease-modifying antirheumatic drugs (DMARDs) has greatly contributed to the improvement of patients' symptoms, such as pain and swelling, but most of the antirheumatic drugs were originally developed to suppress immune reactions. Consequently, many patients experience severe bone destruction and undergo joint replacement surgery in spite of long-term use of immunosuppressive drugs. Thus, it is widely accepted that antirheumatic drugs should have the capacity to suppress bone destruction (2,3).

Several lines of evidence indicate that bone destruction in arthritis is mainly mediated by bone-resorbing osteoclasts, and enhanced expression of receptor activator of NF-κB ligand (RANKL) is responsible for the aberrant activation of osteoclastogenesis in inflammatory lesions. First, RANKL is highly expressed by synovial fibroblasts and T cells in arthritic joints, and the soluble decoy receptor for RANKL, osteoprotegerin (OPG), inhibits osteoclastogenesis both in vitro and in vivo (4–7). Second, bone destruction in arthritis was greatly reduced in *RANKL*$^{-/-}$ mice or *Fos*$^{-/-}$ mice, both of which lack osteoclasts (8,9). Finally, it is notable that antiosteoclast therapy successfully ameliorated bone damage in several models of inflammatory bone destruction (4,10,11). Thus, inhibition of RANKL-mediated osteoclastogenesis may be one of the ideal means to control bone destruction in arthritis (12).

In arthritis, T cells are involved in several pathways that lead to bone damage (3). Aberrant activation of the immune system in arthritic synovium induces macrophage-derived proinflammatory cytokines, such as tumor necrosis factor α (TNFα) and interleukin-1 (IL-1), which strongly induce RANKL on synovial fibroblasts (5,13,14). To induce bone-associated pathogenic conditions, T cells are involved in the initiation and exacerbation of this synovitis. The importance of this pathway is underscored by the observation that the neutralization of these cytokines has significant therapeutic effects on bone destruction (2,3). In addition, activated T cells expressing RANKL may contribute directly to osteoclastogenesis (4). Consequently, the level of RANKL induced by both synovial fibroblasts and T cells becomes too high to be counterbalanced by inhibitors such as interferon-γ (IFNγ) or OPG (4,13). Although some antirheumatic drugs have bone-protective effects (15,16), this complex mechanism of bone damage makes it difficult to understand the molecular basis of these protective effects.

Leflunomide is a DMARD of the isoxazole class, and it inhibits de novo pyrimidine biosynthesis by acting on dihydroorotate dehydrogenase (DHODH) (15,17). It has a protective effect against bone damage in animal models and in humans (17–19), and it has recently been introduced for the treatment of RA (15,17). It was previously reported that leflunomide suppresses proliferation or activation of T cells (20), and it has also been introduced as an immunosuppressive drug in the transplantation of allografts (21). However, it is currently unknown if leflunomide acts directly on the lineage of bone-resorbing osteoclasts.

NF-ATc1, also referred to as NF-AT2 or NF-ATc, is a member of the NF-AT (nuclear factor of activated T cells) family of transcription factors, originally discovered in the context of the activation of the immune system (22). Members of the NF-AT family are also involved in the function and development of diverse cells in other biologic systems, including cardiovascular and musculoskeletal systems in vertebrates, where they are under the control of a Ca^{2+}-regulated phosphatase, calcineurin (23). Importantly, we have recently discovered that NF-ATc1 is strongly induced by RANKL and plays a central role in RANKL-induced osteoclast differentiation (24). Thus, NF-ATc1 may be a good therapeutic target in osteoclast-mediated osteopenic diseases, including RA.

In this study, we show that leflunomide acts directly on the osteoclast precursor cells of monocyte/macrophage lineage. Evidence is provided to show that leflunomide selectively inhibits RANKL-induced differentiation of osteoclasts by interfering with de novo pyrimidine synthesis and the Ca^{2+}–NF-ATc1 pathway. We further demonstrate that leflunomide has a bone-protective effect on an endotoxin-induced bone destruction model in mice deficient in the *rag-2* gene, which indicates that the bone-protective effect of leflunomide is, at least in part, independent of T cells. Our results reveal a new aspect of this antirheumatic drug and provide evidence of an interesting interrelationship between Ca^{2+} signaling and de novo pyrimidine biosynthesis.

MATERIALS AND METHODS

In vitro differentiation of osteoclasts. The osteoclast formation system has been described previously (13,25). Briefly, nonadherent bone marrow cells derived from C57BL/6 mice were seeded (5×10^4 cells per well in a 24-well plate, 1.5–2.0 × 10^7 cells in a 10-cm dish) and cultured in α-minimum essential medium (α-MEM; Gibco BRL, Grand Island, NY) with 10% fetal bovine serum (FBS; Sigma, St. Louis, MO) containing 10 ng/ml macrophage colony-stimulating factor (M-CSF; Genzyme, Cambridge, MA). Bone marrow monocyte/

macrophages (BMMs) were maintained with this concentration of M-CSF in all experiments. After 2 days, adherent cells were used as BMMs after washing out the nonadherent cells including lymphocytes. BMMs were further cultured in the presence of 100 ng/ml soluble RANKL (PeproTech, Rocky Hill, NJ) and 10 ng/ml M-CSF to generate osteoclasts. To evaluate the effect of leflunomide, an active metabolite of leflunomide (A77 1726, a gift from Aventis Pharmaceuticals, Bridgewater, NJ) was added at the same time as RANKL unless otherwise described. Three days later, tartrate-resistant acid phosphatase (TRAP)–positive multinucleated (>3 nuclei) cells (TRAP+ MNCs) were counted. RAW 264.7 cells (2.5×10^4 cells per well in a 24-well plate) were stimulated with RANKL (100 ng/ml) in the presence or absence of leflunomide. After 5 days, TRAP+ MNCs were counted. TRAP+ MNCs were characterized by examining the bone-resorbing activity on dentine slices and the expression of calcitonin receptors, as previously described (13). The experiments in this study were approved by the institutional committee on animal experiments.

In vitro differentiation of osteoblasts. Osteoblasts were isolated from the calvaria of newborn (3–5 days old) mice by enzymatic digestion in 0.1% collagenase and 0.2% dispase, and were cultured in α-MEM with 10% FBS. After 2 days, cells were reseeded (5×10^4 cells per well in a 24-well dish), and cultured in α-MEM with 10% FBS containing 50 μg/ml ascorbic acid, 10 m*M* sodium β-glycerophosphate, and 10 n*M* dexamethasone, in the presence or absence of leflunomide (30 μ*M*), as previously described (25).

Extraction and high-performance liquid chromatography (HPLC) assay of ribonucleotides. The extraction and assay of ribonucleotides have been previously described (26). Briefly, BMMs were stimulated with RANKL (100 ng/ml) and M-CSF (10 ng/ml) in the presence or absence of leflunomide (50 μ*M*). After 24 hours, cells were deproteinized with 10% trichloroacetic acid (TCA). The cell extracts were then centrifuged for 1 minute at 12,000*g*, and the TCA in the supernatants was removed by back extraction with water-saturated diethyl ether to pH 5. The extracts were examined by HPLC assay.

Activation of MAP kinases, Akt, and NF-κB. BMMs, preincubated in the presence or absence of leflunomide (30 μ*M*) for 24 hours, were stimulated with RANKL and analyzed by immunoblotting using antiphosphorylated MAP kinase, anti–MAP kinase, antiphosphorylated Akt, or anti-Akt antibodies (New England Biolabs, Beverly, MA), as previously described (13,25). For an electrophoretic mobility shift assay, BMMs were preincubated in the presence or absence of leflunomide (30 μ*M*) for 24 hours. After RANKL stimulation, a cell extract was prepared and analyzed using an oligonucleotide probe containing the NF-κB binding site of the IFNγ promoter, as previously described (13,25). Supershift was performed with an anti-RelA antibody (Santa Cruz Biotechnology, Santa Cruz, CA).

Gene analysis. Genome-wide screening was performed using essentially the same system as previously described (24). Briefly, BMMs were stimulated with RANKL (100 ng/ml) and M-CSF (10 ng/ml) in the presence or absence of leflunomide (100 μ*M*). After 24 hours, total RNA was extracted from BMMs using a Sepasol RNA extraction kit (Nacalai Tesque, Kyoto, Japan). Total RNA (15 μg) was utilized for complementary DNA synthesis by reverse transcription, followed by synthesis of biotinylated complementary RNA (cRNA) by in vitro transcription. After cRNA fragmentation, hybridization with mouse U74Av2 GeneChip arrays (Affymetrix, Santa Clara, CA) displaying probes for 12,000 mouse genes/expressed sequence tags was performed according to the manufacturer's protocol. Chips were washed, stained with streptavidin–phycoerythrin, and analyzed using the Affymetrix GeneChip scanner and accompanying gene expression software.

Immunoblot analysis and immunofluorescence staining. To evaluate expression of downstream molecules of RANKL signaling during osteoclastogenesis, BMMs were stimulated with RANKL/M-CSF in the presence or absence of leflunomide (30 μ*M*). Whole-cell lysate of BMMs was examined every 24 hours after the addition of RANKL by immunoblot analysis using specific antibodies for NF-ATc1 (7A6), tumor necrosis factor receptor–associated factor 6 (TRAF6) (H-274), and c-Fos (H-125) (Santa Cruz Biotechnology). For immunostaining, cells were cultured with RANKL/M-CSF for 3 days in the presence or absence of leflunomide (30 μ*M*), fixed in 4% paraformaldehyde for 20 minutes, and treated with 0.2% Triton X-100 for 5 minutes. Cells were sequentially incubated in 5% bovine serum albumin/phosphate buffered saline (PBS) for 30 minutes, 2 μg/ml anti–NF-ATc1 antibody and 4 μg/ml anti–c-Fos (or anti-TRAF6) antibody in PBS–Tween for 60 minutes, and then 4 μg/ml Alexa Fluor 488 or 8 μg/ml Alexa Fluor 546–labeled secondary antibodies (Molecular Probes, Eugene, OR) for 60 minutes. For immunostaining of DHODH, BMMs or mature osteoclasts were incubated with 500 n*M* MitoTracker Orange (Molecular Probes) for 20 minutes and fixed as described above. Cells were sequentially incubated with rabbit anti-DHODH polyclonal IgG (27,28), and then with 4 μg/ml Alexa Fluor 488–labeled secondary antibody.

Retroviral gene transfer. The retroviral vectors pMX-NF-ATc1-IRES-EGFP (pMX-NF-ATc1), pMX-c-fos-IRES-EGFP (pMX-c-fos), and pMX-TRAF6-IRES-EGFP (pMX-TRAF6) have been previously described (13,24,25). Retrovirus packaging was performed by cotransfection of these pMX vectors and pPAMpsi2 (a gift from C. L. Sawyers) into 293T cells. Two days after inoculation, BMMs were stimulated with RANKL/M-CSF plus leflunomide (30 μ*M*). Osteoclastogenesis was evaluated 3 days after RANKL addition by TRAP staining and bone resorption assay, as previously described (13).

Ca^{2+} measurement. BMMs were incubated with RANKL/M-CSF for 48 hours in the presence or absence of leflunomide (30 μ*M*). Cells were loaded with calcium indicators (fluo-4 AM; Molecular Probes) and analyzed by confocal microscopy (C1; Nikon, Tokyo, Japan), as previously described (24). The increase in the ratio of fluorescence intensity from the basal level was divided by the maximum increase in the ratio obtained by adding 10 μ*M* ionomycin, and was expressed as the percentage maximum ratio increase.

Endotoxin-induced bone resorption. *Rag-2*$^{-/-}$ mice (Taconic, Germantown, NY) have been previously described (29). Mice, 7 weeks old (n = 10), were administered a local calvarial injection of lipopolysaccharide (LPS; Sigma) at 25 mg/kg body weight, as previously described (25,30). Mice were treated with a single injection of leflunomide (10 mg/kg body weight) or saline at the site of the LPS injection. After 5 days, calvarial tissues were embedded and frozen in 5% carboxymethylcellulose (CMC) sodium, and serial sections were stained for TRAP (with hematoxylin) and NF-ATc1, as previ-

ously described (24). Parameters such as the osteoclast number per millimeter of trabecular bone surface and the number of NF-ATc1–positive cells were determined.

NF-ATc1 expression in RA tissues. With informed consent, tissues were obtained from the bone–synovium interface of RA patients who underwent knee joint replacement surgery because of severe bone destruction (n = 4). The samples were embedded and frozen in CMC sodium and analyzed as described above.

Statistical analysis. All data are expressed as the mean ± SEM (n = 6). All experiments were repeated more than 3 times throughout the study. Statistical analysis was performed using Student's *t*-test.

RESULTS

Inhibition of RANKL-induced osteoclastogenesis by restriction of pyrimidine synthesis. To determine whether leflunomide acted directly on osteoclast differentiation (and, if so, how), we first examined the effect of leflunomide on in vitro osteoclast formation from BMMs stimulated with RANKL in the presence of M-CSF. As shown in Figure 1a, leflunomide strongly inhibited the formation of TRAP+ MNCs in a dose-dependent manner (1–100 μM). The survival and proliferation of BMMs were not significantly affected by a low concentration of leflunomide, but higher concentrations of leflunomide had a suppressive effect on the proliferation of BMMs (Figure 1b), which was much less than that on osteoclast differentiation. In addition, a similar inhibitory effect was observed in RANKL-induced osteoclastogenesis of RAW 264.7 cells, which are independent of M-CSF, suggesting that leflunomide inhibits osteoclast differentiation by interfering with RANKL signaling (Figure 1c).

In the de novo pyrimidine synthesis pathway, DHODH is a critical enzyme that converts dihydroorotate into orotic acid, which is essential for the synthesis of UMP, which is phosphorylated to UTP (26). The inhibitory effect of leflunomide (concentrations of 30 μM or less) on osteoclast differentiation was completely reversed by the addition of an excessive amount of uridine, suggesting that the blockade of de novo uridine synthesis is responsible for this inhibition (Figures 1a and d). The inhibition was only partially reversed at 100 μM of leflunomide, suggesting a nonpyrimidine-related effect at higher concentrations. We also examined the stage at which the osteoclast formation process is inhibited by the presence of leflunomide during RANKL stimulation. The formation of TRAP+ MNCs was almost completely inhibited when leflunomide was added at an early stage, i.e., between 0 and 24 hours after RANKL stimulation, whereas such inhibition was not

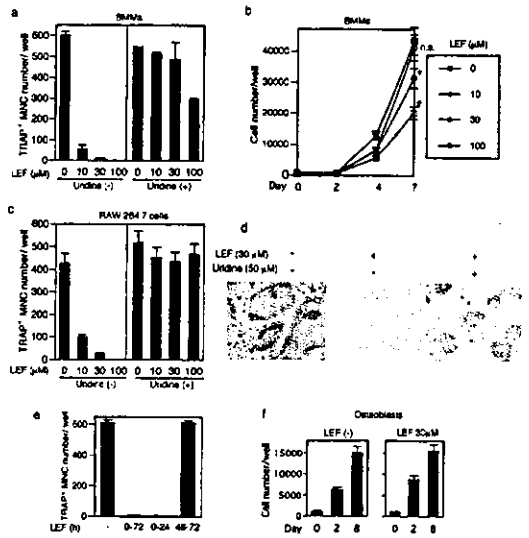

Figure 1. Effect of leflunomide (LEF) on receptor activator of NF-κB ligand (RANKL)–induced osteoclastogenesis. **a**, LEF inhibited the formation of tartrate-resistant acid phosphatase (TRAP)–positive multinucleated cells (TRAP+ MNCs) from bone marrow monocyte/macrophages (BMMs) stimulated with RANKL in the presence of macrophage colony-stimulating factor (M-CSF). This inhibition was reversed by the addition of uridine (50 μM). **b**, Effect of LEF on the proliferation and survival of BMMs stimulated with M-CSF. * = $P < 0.05$; # = $P < 0.01$, versus proliferation with no LEF added. n.s. = not significant. **c**, Effect of LEF on the formation of TRAP+ MNCs from RAW 264.7 cells stimulated with RANKL. This inhibition was reversed by the addition of uridine (50 μM). **d**, Photomicrograph of in vitro osteoclast differentiation from BMMs (TRAP staining). The inhibitory effect of LEF was reversed by uridine. **e**, Differentiation stage–dependence of the effect of LEF. The addition of LEF (30 μM) at the early stage (0–24 hours) completely inhibited osteoclastogenesis, but addition at the late stage (48–72 hours) had no effect. **f**, Effect of LEF on the proliferation and differentiation of osteoblasts. LEF had no significant effect on the increase in the number of cultured osteoblasts. Values are the mean ± SEM.

observed when the drug was added 48 hours after RANKL stimulation (Figure 1e). These results indicated that leflunomide suppresses cellular events that are activated by RANKL at an early stage of osteoclast differentiation.

On the other hand, when we examined the effect of leflunomide on the proliferation (Figure 1f) and differentiation (data not shown) of osteoblasts, in which RANKL signaling is not involved, little, if any, inhibitory effect was observed. These results showed that leflunomide selectively acts on the RANKL-dependent osteoclast differentiation process.

The importance of pyrimidine synthesis in

RANKL signaling suggests that DHODH, which is a critical enzyme for de novo pyrimidine synthesis and the known target of leflunomide, is induced by RANKL in osteoclast precursor cells. Using GeneChip analysis, we determined the level of messenger RNA (mRNA) for DHODH in BMMs stimulated with RANKL. As shown in Figure 2a, the level of DHODH mRNA was increased by RANKL. Furthermore, immunostaining was performed using an anti-DHODH antibody (28) and DHODH was found to be abundantly expressed by mature osteoclasts as well as by BMMs. Consistent with previous reports on other cell types (27), expression of DHODH was mainly observed in mitochondria (Figure 2b). Furthermore, using HPLC analysis, the concentration of pyrimidine ribonucleotides, including UMP and CMP, was evaluated in RANKL-stimulated BMMs. The concentration of all pyrimidines was decreased by the addition of leflunomide (Figure 2c), indicating that pyrimidine biosynthesis is actually suppressed by leflunomide in RANKL-stimulated BMMs, as seen in T cells (26). Collectively, these results suggest that de novo pyrimidine synthesis is important for RANKL-induced osteoclast differentiation, and leflunomide inhibits this process by targeting DHODH in osteoclast lineage.

Effect of leflunomide on downstream signaling pathways activated by RANKL. These results prompted us to investigate the mechanism by which leflunomide interferes with the intracellular signaling pathways activated by RANKL. Briefly, RANKL signals the cell by binding with its receptor, RANK, resulting in the activation of TRAF family proteins such as TRAF6, which activates the NF-κB, MAP kinase, and Akt pathways (6,13,31). RANKL also induces c-Fos, which may function in the context of the activator protein 1 transcription factor complex (25,32,33). RANKL selectively induces the *NF-ATc1* gene in a TRAF6- and c-Fos–dependent manner (24). RANKL also evokes Ca^{2+} signaling, which leads to calcineurin-mediated activation of NF-ATc1, and this activation is necessary and sufficient for osteoclast differentiation (24).

To explore the molecular basis of leflunomide inhibition of osteoclastogenesis, we examined its effect on RANKL-induced activation of these downstream signaling molecules. As shown in Figure 3a, an inhibitory effect was not observed in the RANKL-induced activation of MAP kinases, including ERK, p38, and JNK, in leflunomide-treated BMMs. In addition, leflunomide had little, if any, effect on RANKL-induced activation of NF-κB (Figure 3b) and Akt (Figure 3c), suggesting that these molecules may not be the targets of leflunomide action on RANKL signaling.

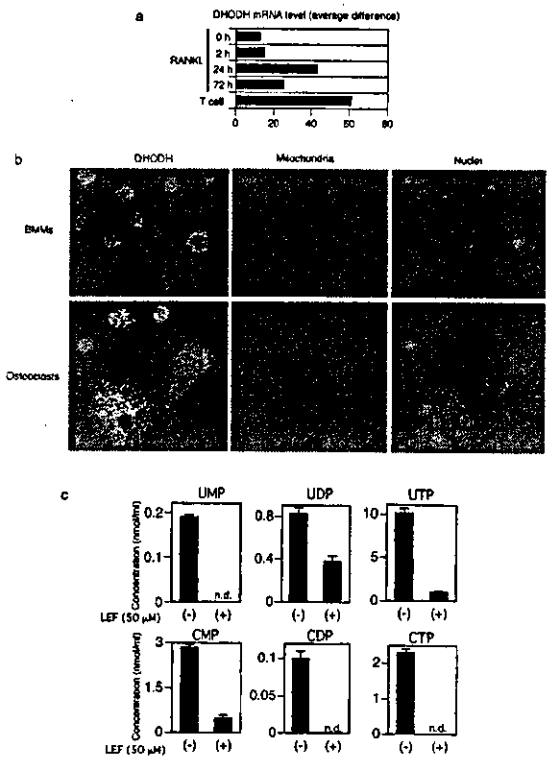

Figure 2. Expression of dihydroorotate dehydrogenase (DHODH) in the osteoclast lineage and its inhibition by LEF. **a**, Expression of DHODH mRNA in RANKL-stimulated BMMs. Expression of mRNA was detectable in unstimulated BMMs, and it was enhanced by RANKL stimulation. The induction level was comparable with that of splenic T cells. GeneChip analysis was repeated 3 times and yielded similar results; a representative set of data is shown. **b**, Immunocytochemical localization of the DHODH protein in osteoclast precursor cells and osteoclasts. DHODH was abundantly expressed in mature osteoclasts as well as in BMMs. DHODH expression was mainly observed in the mitochondria as visualized by MitoTracker Orange. Nuclei were stained with Hoechst 33342. **c**, High-performance liquid chromatography analysis of the intracellular concentration of pyrimidine nucleotides in RANKL-stimulated BMMs. In the presence of LEF, the concentration of pyrimidines was greatly down-regulated. Values are the mean and SEM. n.d. = not detectable (see Figure 1 for other definitions).

Identification of NF-ATc1 as a specific target of leflunomide action. To gain insights into the molecular targets of leflunomide, we performed a genome-wide screening of RANKL-inducible genes in BMMs stimulated with RANKL in the presence or absence of leflunomide. We utilized GeneChip arrays and analyzed the mRNA expression of transcription factors and effector molecules, which are involved in RANKL signaling

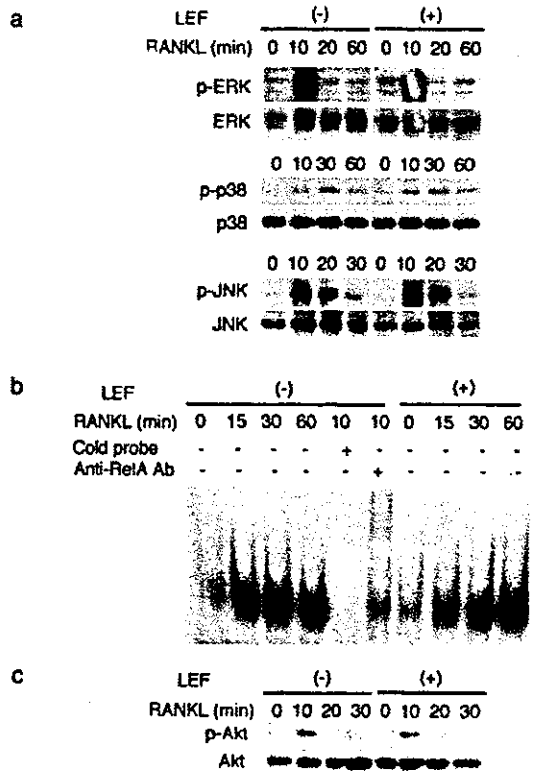

Figure 3. Effect of LEF on RANKL-activated signaling pathways. **a**, LEF had no significant effect on RANKL-induced activation of p38, ERK, or JNK in BMMs. The BMMs were incubated with LEF for 24 hours and stimulated with RANKL (100 ng/ml) in the presence of M-CSF (10 ng/ml). Whole-cell lysate was recovered after the indicated periods. **b**, Effect of LEF on RANKL-induced activation of NF-κB in BMMs. LEF had little, if any, effect on the formation of NF-κB complex. The band of NF-κB complex was shifted by the addition of anti-RelA antibody (Ab). **c**, Activation of Akt by RANKL was not affected by LEF. p-ERK = phosphorylated ERK; p-p38 = phosphorylated p38; p-JNK = phosphorylated JNK; p-Akt = phosphorylated Akt (see Figure 1 for other definitions).

(Figure 4). Interestingly, a selective suppressive effect of leflunomide was observed on the transcription factor NF-ATc1. As shown in Figure 4, the expression of *NF-ATc1* mRNA was increased >20-fold by RANKL, but the addition of leflunomide reduced this expression markedly (>80% inhibition), whereas expressions of other genes were not significantly affected under this experimental condition.

As expected from the above result, leflunomide strongly inhibited the RANKL induction of NF-ATc1 protein (Figure 5a). In addition, the induction levels of TRAF6 and c-Fos also decreased, particularly at the late stage (3 days after RANKL stimulation), but they were still observed. Consistently, NF-ATc1 expression in

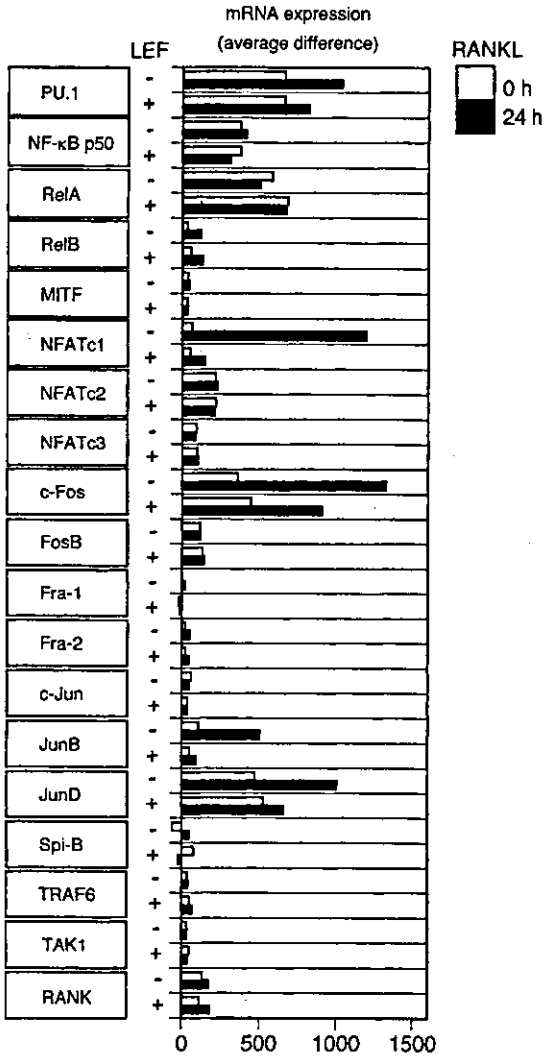

Figure 4. Genome-wide screening of targets of LEF action in RANKL-inducible genes: mRNA expression level (average difference) of genes encoding transcription factors and molecules involved in RANKL signaling. BMMs were stimulated with RANKL for 24 hours in the presence or absence of LEF, and mRNA expression was analyzed by GeneChip analysis. GeneChip analysis was repeated several times and yielded similar results; a representative set of data is shown. MITF = microphthalmia transcription factor; NF-ATc1 = nuclear factor of activated T cells c1; TRAF6 = tumor necrosis factor receptor–associated factor 6; TAK-1 = transforming growth factor β-activated kinase 1 (see Figure 1 for other definitions).

BMMs stimulated with RANKL in the presence of leflunomide was barely detected by immunostaining, but the expression of c-Fos or TRAF6 was still observed, albeit at lower levels, under the same conditions (Figure 5b).

Effect of leflunomide on the RANKL-stimulated NF-ATc1 induction pathway. The above results collectively suggest that restriction of uridine synthesis, which would generally be required for RNA synthesis, selectively suppresses the NF-ATc1 induction pathway stimulated with RANKL. It has been shown that RANKL-induced Ca^{2+} oscillation is essential for the autoamplification of *NF-ATc1* gene expression that is critical the sustained NF-ATc1–dependent transcriptional (24). We therefore examined the effect of leflunomide on Ca^{2+} signaling in BMMs stimulated with RANKL. Interestingly, as shown in Figure 5c, Ca^{2+} oscillation induced by RANKL was inhibited by leflunomide, suggesting that the inhibition of RANKL-induced Ca^{2+} signaling accounts for the inhibition of NF-ATc1 expression by leflunomide.

If the inhibition of RANKL-induced Ca^{2+} signaling and NF-ATc1 induction is the critical target of leflunomide, one would expect that the leflunomide-mediated inhibition of osteoclast differentiation would be overcome by ectopic NF-ATc1 expression. To address this issue, we examined the effect of ectopic expression of NF-ATc1, TRAF6, or c-Fos on the suppressive action of leflunomide by retrovirus-mediated gene transfer (24). Interestingly, ectopic expression of NF-ATc1, but not c-Fos or TRAF6, resulted in efficient osteoclast formation even in the presence of leflunomide (Figure 5d). These results lend further support for the notion that leflunomide exerts a selective action on the RANKL-induced Ca^{2+}/NF-ATc1 pathway.

T cell–independent effect of leflunomide on inflammatory bone destruction. Leflunomide exerts its immunosuppressive effect by acting on T cells, but it is difficult to segregate T cell–dependent immunosuppressive effects from T cell–independent effects in the in vivo mechanism of leflunomide action. To determine whether leflunomide exerts its protective effect on bone through a T cell–independent mechanism, we developed a model of inflammatory bone destruction that is induced in the absence of T cells. LPS was injected into the calvaria of mice deficient in the *rag-2* gene (*rag-2*$^{-/-}$ mice), which lack both T and B cells (29). It has been shown that injection of a low dose of LPS does not induce bone destruction in T cell–deficient nude mice (34), but we successfully induced bone destruction in *rag-2*$^{-/-}$ mice using a high dose of LPS, indicating

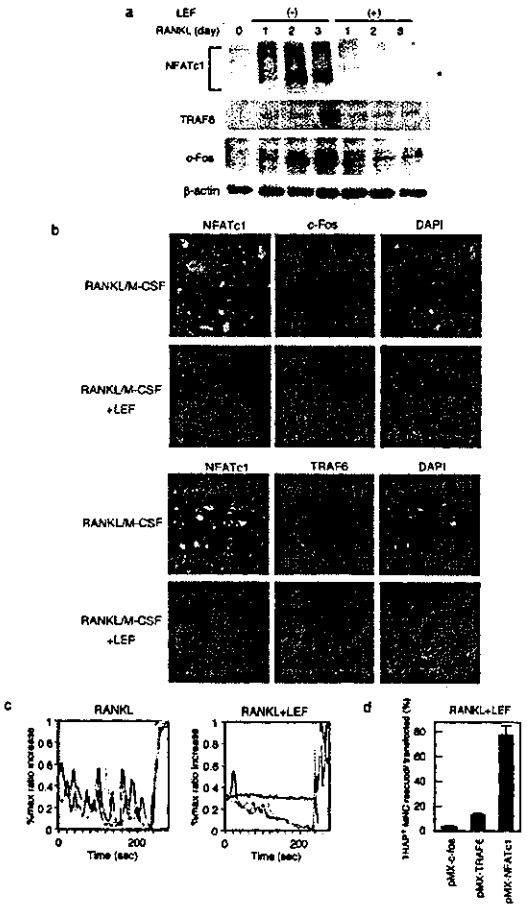

Figure 5. Inhibition of RANKL signaling by LEF through down-regulation of nuclear factor of activated T cells c1 (NF-ATc1) pathway. **a,** Effect of LEF on the expression of essential mediators of RANKL signaling. NF-ATc1 was markedly induced by RANKL and became dephosphorylated (**asterisk**) in the course of differentiation. LEF had a strong inhibitory effect on NF-ATc1 expression. **b,** Expression of c-Fos, tumor necrosis factor receptor–associated factor 6 (TRAF6), and NF-ATc1 in BMMs stimulated with RANKL in the presence or absence of LEF. **c,** Effect of LEF on Ca^{2+} signaling in BMMs induced by RANKL. $[Ca^{2+}]i$ change in single cells was detected by loading Ca^{2+} indicators. Each color indicates a different cell in the same field. **d,** Effect of retroviral overexpression of c-Fos, TRAF6, and NF-ATc1 on the inhibitory effect of LEF. Values are the mean and SEM. DAPI = 4′,6-diamidino-2-phenylindole (see Figure 1 for other definitions).

that lymphocytes are dispensable in this model system (Figure 6a).

Interestingly, when these mice received locally administered leflunomide, bone destruction and exces-

sive osteoclast formation were significantly ameliorated (Figures 6a and b). It was notable that a considerable number of TRAP+ MNCs in inflammatory lesions stained positively for NF-ATc1 (Figure 6a), and this was substantially reduced following treatment with leflunomide (Figure 6b). In contrast, expression of other members of the NF-AT family, such as NF-ATc2, was barely detected (results not shown). Thus, leflunomide has an antiosteoclastogenic effect in vivo, which is not targeted at T cells. Although we cannot rule out the possibility that leflunomide also acts on other cell types, our results were consistent with the above in vitro results, showing the direct inhibitory effect of leflunomide on osteoclast precursor cells by interfering with NF-ATc1 expression. Consistently, leflunomide had only a marginal effect on inflammatory reactions in *rag*-$2^{-/-}$ mice (Figure 6c and data not shown). In contrast, when wild-type mice were treated with leflunomide in an LPS-induced bone destruction model, we observed a suppressive effect on inflammatory reactions and a more powerful suppressive effect on osteoclast formation than that in *rag*-$2^{-/-}$ mice (results not shown), suggesting that the bone-protective effect of leflunomide in vivo is partially due to its suppressive effect on T cells.

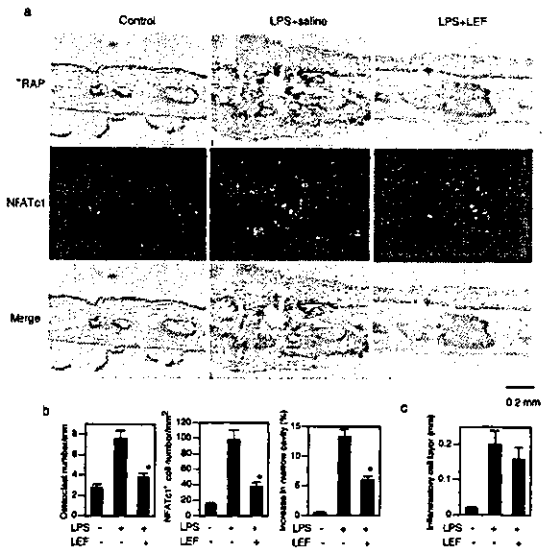

Figure 6. Effect of LEF on a T cell–independent model of inflammatory bone destruction in *rag*-$2^{-/-}$ mice. **a**, Lipopolysaccharide (LPS) induced enhanced osteoclast formation and inflammation-related bone resorption in *rag*-$2^{-/-}$ mice. Note that bone destruction was accompanied by an increase in the number of TRAP-positive and nuclear factor of activated T cells c1 (NF-ATc1)–positive cells. LEF ameliorated this bone resorption significantly. **b**, Effect of LEF on bone resorption parameters, such as osteoclast number, NF-ATc1–positive cell number, and increase in area of marrow cavity. * = $P <$ 0.05 versus saline-only treatment. **c**, Effect of LEF on formation of an inflammatory cell layer. Values are the mean and SEM. See Figure 1 for other definitions.

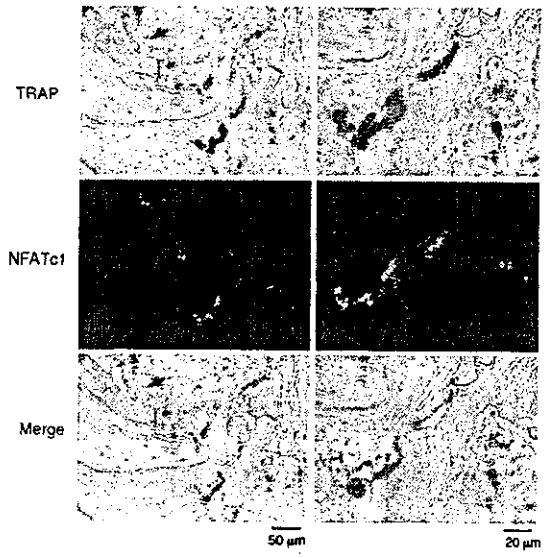

Figure 7. Expression of nuclear factor of activated T cells c1 (NF-ATc1) in osteoclasts in rheumatoid arthritis (RA). TRAP+ MNCs at the bone–synovium interface in RA patients were positive for NF-ATc1. Similar results were obtained in all samples. The right panel shows a magnified view of bone-resorbing osteoclasts, which expressed a high level of NF-ATc1 in arthritic joints. See Figure 1 for other definitions.

It is important to evaluate whether NF-ATc1 expression is up-regulated in RA tissues. In this regard, it is interesting that selective and strong expression of NF-ATc1 was observed in multinucleated osteoclasts at the bone–synovium interface in patients with RA (Figure 7).

DISCUSSION

Bone destruction in RA is initially triggered by the activation of T cells, which eventually enhances the expression of RANKL in synoviocytes, as well as in T cells themselves (4,5,13). Inflammatory cytokines also contribute to this pathogenesis by increasing the expression and activity of RANKL (6,13). Thus, there are several strategies by which to suppress bone destruction: suppression of T cell activation, inhibition of osteoclast formation/function, or blockade of inflammatory cytokines. Leflunomide has an effective therapeutic action

on animal models of autoimmune arthritis, and randomized controlled studies in human RA revealed that leflunomide is one of the antirheumatic drugs that reduces the progression of bone damage (17–19). Leflunomide has been thought to ameliorate the course of arthritis by its inhibitory effect on T cells, but we found that it has a marked suppressive effect on RANKL-activated intracellular signaling and osteoclast differentiation. Using a bone destruction model in the absence of T cells, we showed that the effect of leflunomide is also targeted at osteoclastogenesis directly, extending beyond its suppressive effect on T cells. Given the central role of RANKL in arthritic bone destruction, antirheumatic drugs that inhibit RANKL signaling, such as leflunomide, will contribute to the maintenance of joint structure through the direct inhibition of bone-resorbing osteoclasts.

Is osteoclastogenesis in RA dependent on T cells or not? As described above, T cells play important roles as an initial trigger and as a constant stimulator of bone destruction, mainly by inducing inflammatory cytokines (e.g., TNFα, IL-1) and RANKL on synovial fibroblasts. Although RANKL is expressed on T cells (4), T cells also produce the inhibitors of RANKL, such as IFNγ (13). Thus, the relative contribution of RANKL in these cell types remains elusive. But LPS-induced bone destruction or collagen-induced arthritis can be induced in mice lacking T cells (35). Therefore, T cell–mediated reactions are not essential for osteoclastogenesis in some models of inflammatory bone destruction. Although T cells contribute greatly to the pathogenesis of bone destruction in RA, the enhanced expression of RANKL on synoviocytes induced by synovial inflammation may be a critical molecular basis for osteoclastogenesis in arthritis. Activation of T cells should be one of the initiators of this inflammation, but RANKL on T cells may not be essential for osteoclastogenesis in inflammatory lesions. Further studies are necessary to determine in more detail how T cells contribute to osteoclastogenesis in RA.

A genome-wide screening of RANKL-inducible genes using GeneChip made it possible for us to identify the transcription factor NF-ATc1 as a selective target of leflunomide action. We found that induction of the *JunB* gene is also affected by leflunomide. However, it is reported that Jun family members play redundant roles in hematopoietic cells (36), suggesting that decreased expression of JunB cannot explain the strong suppressive effect of leflunomide on osteoclastogenesis. This is further supported by the observation that the inhibitory effect of leflunomide on osteoclastogenesis is specifically reversed by ectopic expression of NF-ATc1. Since expression of both TRAF6 and c-Fos proteins was reduced by the addition of leflunomide at a late stage, we cannot rule out the possibility that the action of leflunomide is partly mediated through its effect on other molecules such as TRAF6 and c-Fos.

Our results raise an interesting issue of how blocking de novo pyrimidine biosynthesis selectively affects the RANKL-induced Ca^{2+} signaling pathway. In fact, purine and pyrimidine nucleotides are generally important for cellular functions. In addition, they play important roles as extracellular signaling molecules (37). For example, it has been shown that UTP and ATP evoke Ca^{2+} signaling through binding with nucleotide receptors such as P2X and P2Y (37–39). It is interesting that these receptors are expressed by cells of the osteoclast lineage (40,41), and we also detected expression of P2X7 and P2X4 in bone marrow–derived osteoclast precursor cells during osteoclastogenesis (Takayanagi H: unpublished observations). Since the mechanism by which RANKL stimulation results in Ca^{2+} oscillation is currently unknown (23), further studies will be required to determine the detailed mechanism by which the restriction of de novo pyrimidine synthesis is linked to RANKL-induced Ca^{2+} oscillation.

We demonstrated that NF-ATc1 expression is actually enhanced in inflammatory tissues adjacent to sites of bone destruction and is down-regulated by leflunomide treatment in animal models. To focus on the effect of leflunomide on bone destruction, but not on the immune system, we used the LPS-induced bone destruction model, which mimics the destructive phase of arthritis, instead of using models such as collagen-induced arthritis. We also showed that NF-ATc1 is strongly expressed in multinucleated osteoclasts at the bone–synovium interface in patients with RA, indicating the possibility that up-regulation of NF-ATc1 expression may be a feature shared among various bone-destructive or metabolic bone diseases. Although the correlation between NF-AT expression and disease severity is an issue that remains to be examined, colocalization of NF-ATc1 with TRAP suggests that NF-AT expression may also be related to severe RA with abundant TRAP+ MNCs, which actively resorb bone. Considering the specific effect of leflunomide on NF-ATc1 induction and the abundance of NF-ATc1 in osteoclasts, leflunomide should be a good therapeutic agent for suppressing osteoclastogenesis in arthritis. Suppression of the NF-ATc1 pathway would be an advantageous strategy against bone destruction in arthritis characterized by enhanced osteoclastogenesis. It is also beneficial for

suppressing steroid-induced osteoporosis that is often observed in RA patients.

We have previously reported that calcineurin inhibitors, such as FK-506 and cyclosporin A, have strong inhibitory effects on osteoclastogenesis (24). It is notable that FK-506 is also in clinical trials for the treatment of RA, with promising results (42). Methotrexate is one of the most widely used antirheumatic drugs that have a bone-protective effect. Methotrexate also has a direct suppressive effect on osteoclastogenesis (Urushibara M, Takayanagi H: unpublished observations), suggesting that bone-protective antirheumatic drugs may have a direct effect on osteoclast lineage in common. Our preliminary data also show that leflunomide and FK-506 have synergistic inhibitory effects on osteoclastogenesis (Urushibara M, Takayanagi H: unpublished observations). Therefore, a combination of antiosteoclastogenic drugs may be a promising approach to augmenting efficacy and also may reduce the possibility of side effects in the treatment of bone destruction in RA.

ACKNOWLEDGMENTS

We thank Aventis Pharmaceuticals for providing the leflunomide metabolite, and T. Yokochi and A. Suematsu for invaluable suggestions and technical help. We also thank K. Sato, M. Asagiri, M. Isshiki, A. Takaoka, K. Honda, S. Kano, C. Nakajima, S. Tanaka, H. Oda, K. Nakamura, and I. Kawai for their assistance and discussions.

REFERENCES

1. Feldmann M, Brennan FM, Maini RN. Rheumatoid arthritis. Cell 1996;85:307–10.
2. Feldmann M, Maini RN. Anti-TNFα therapy of rheumatoid arthritis: what have we learned? Annu Rev Immunol 2001;19: 163–96.
3. Choy EH, Panayi GS. Cytokine pathways and joint inflammation in rheumatoid arthritis. N Engl J Med 2001;344:907–16.
4. Kong YY, Feige U, Sarosi I, Bolon B, Tafuri A, Morony S, et al. Activated T cells regulate bone loss and joint destruction in adjuvant arthritis through osteoprotegerin ligand. Nature 1999; 402:304–9.
5. Takayanagi H, Iizuka H, Juji T, Nakagawa T, Yamamoto A, Miyazaki T, et al. Involvement of receptor activator of nuclear factor κB ligand/osteoclast differentiation factor in osteoclastogenesis from synoviocytes in rheumatoid arthritis. Arthritis Rheum 2000;43:259–69.
6. Theill LE, Boyle WJ, Penninger JM. RANK-L and RANK: T cells, bone loss, and mammalian evolution. Annu Rev Immunol 2002; 20:795–823.
7. Gravallese EM, Manning C, Tsay A, Naito A, Pan C, Amento E, et al. Synovial tissue in rheumatoid arthritis is a source of osteoclast differentiation factor. Arthritis Rheum 2000;43:250–8.
8. Redlich K, Hayer S, Ricci R, David JP, Tohidast-Akrad M, Kollias G, et al. Osteoclasts are essential for TNF-α–mediated joint destruction. J Clin Invest 2002;110:1419–27.
9. Pettit AR, Ji H, von Stechow D, Muller R, Goldring SR, Choi Y, et al. TRANCE/RANKL knockout mice are protected from bone erosion in a serum transfer model of arthritis. Am J Pathol 2001;159:1689–99.
10. Takayanagi H, Juji T, Miyazaki T, Iizuka H, Takahashi T, Isshiki M, et al. Suppression of arthritic bone destruction by adenovirus-mediated csk gene transfer to synoviocytes and osteoclasts. J Clin Invest 1999;104:137–46.
11. Zhao H, Shuto T, Hirata G, Iwamoto Y. Aminobisphosphonate (YM175) inhibits bone destruction in rat adjuvant arthritis. J Orthop Sci 2000;5:397–403.
12. Rodan GA, Martin TJ. Therapeutic approaches to bone diseases. Science 2000;289:1508–14.
13. Takayanagi H, Ogasawara K, Hida S, Chiba T, Murata S, Sato K, et al. T cell-mediated regulation of osteoclastogenesis by signalling cross-talk between RANKL and IFN-γ. Nature 2000;408:600–5.
14. Takayanagi H, Oda H, Yamamoto S, Kawaguchi H, Tanaka S, Nishikawa T, et al. A new mechanism of bone destruction in rheumatoid arthritis: synovial fibroblasts induce osteoclastogenesis. Biochem Biophys Res Commun 1997;240:279–86.
15. Kremer JM. Rational use of new and existing disease-modifying agents in rheumatoid arthritis. Ann Intern Med 2001;134:695–706.
16. Jones G, Halbert J, Crotty M, Shanahan EM, Batterham M, Ahern M. The effect of treatment on radiological progression in rheumatoid arthritis: a systematic review of randomized placebo-controlled trials. Rheumatology (Oxford) 2003;42:6–13.
17. Prakash A, Jarvis B. Leflunomide: a review of its use in active rheumatoid arthritis. Drugs 1999;58:1137–64.
18. Sharp JT, Strand V, Leung H, Hurley F, Loew-Friedrich I, and the Leflunomide Rheumatoid Arthritis Investigators Group. Treatment with leflunomide slows radiographic progression of rheumatoid arthritis: results from three randomized controlled trials of leflunomide in patients with active rheumatoid arthritis. Arthritis Rheum 2000;43:495–505.
19. Cohen S, Cannon GW, Schiff M, Weaver A, Fox R, Olsen N, et al, and the Utilization of Leflunomide in the Treatment of Rheumatoid Arthritis Trial Investigator Group. Two-year, blinded, randomized, controlled trial of treatment of active rheumatoid arthritis with leflunomide compared with methotrexate. Arthritis Rheum 2001;44:1984–92.
20. Breedveld FC, Dayer JM. Leflunomide: mode of action in the treatment of rheumatoid arthritis. Ann Rheum Dis 2000;59:841–9.
21. Williams JW, Mital D, Chong A, Kottayil A, Millis M, Longstreth J, et al. Experiences with leflunomide in solid organ transplantation. Transplantation 2002;73:358–66.
22. Rao A, Luo C, Hogan PG. Transcription factors of the NFAT family: regulation and function. Annu Rev Immunol 1997;15: 707–47.
23. Berridge MJ, Lipp P, Bootman MD. The versatility and universality of calcium signalling. Nat Rev Mol Cell Biol 2000;1:11–21.
24. Takayanagi H, Kim S, Koga T, Nishina H, Isshiki M, Yoshida H, et al. Induction and activation of the transcription factor NFATc1 (NFAT2) integrate RANKL signaling in terminal differentiation of osteoclasts. Dev Cell 2002;3:889–901.
25. Takayanagi H, Kim S, Matsuo K, Suzuki H, Suzuki T, Sato K, et al. RANKL maintains bone homeostasis through c-Fos-dependent induction of IFN-β. Nature 2002;416:744–9.
26. Ruckemann K, Fairbanks LD, Carrey EA, Hawrylowicz CM, Richards DF, Kirschbaum B, et al. Leflunomide inhibits pyrimidine de novo synthesis in mitogen-stimulated T-lymphocytes from healthy humans. J Biol Chem 1998;273:21682–91.
27. Dietz C, Hinsch E, Löffler M. Immunocytochemical detection of mitochondrial dihydroorotate dehydrogenase in human spermatozoa. Int J Androl 2000;23:294–9.
28. Löffler M, Grein K, Knecht W, Klein A, Bergjohann U. Dihydro-

orotate dehydrogenase: profile of a novel target for antiproliferative and immunosuppressive drugs. Adv Exp Med Biol 1998;431: 507–13.
29. Shinkai Y, Rathbun G, Lam KP, Oltz EM, Stewart V, Mendelsohn M, et al. RAG-2-deficient mice lack mature lymphocytes owing to inability to initiate V(D)J rearrangement. Cell 1992;68:855–67.
30. Chiang CY, Kyritsis G, Graves DT, Amar S. Interleukin-1 and tumor necrosis factor activities partially account for calvarial bone resorption induced by local injection of lipopolysaccharide. Infect Immun 1999;67:4231–6.
31. Wong BR, Besser D, Kim N, Arron JR, Vologodskaia M, Hanafusa H, et al. TRANCE, a TNF family member, activates Akt/PKB through a signaling complex involving TRAF6 and c-Src. Mol Cell 1999;4:1041–9.
32. Matsuo K, Owens JM, Tonko M, Elliott C, Chambers TJ, Wagner EF. Fosl1 is a transcriptional target of c-Fos during osteoclast differentiation. Nat Genet 2000;24:184–7.
33. Karsenty G, Wagner EF. Reaching a genetic and molecular understanding of skeletal development. Dev Cell 2002;2: 389–406.
34. Ukai T, Hara Y, Kato I. Effects of T cell adoptive transfer into nude mice on alveolar bone resorption induced by endotoxin. J Periodontal Res 1996;31:414–22.
35. Plows D, Kontogeorgos G, Kollias G. Mice lacking mature T and B lymphocytes develop arthritic lesions after immunization with type II collagen. J Immunol 1999;162:1018–23.
36. Jochum W, Passegue E, Wagner EF. AP-1 in mouse development and tumorigenesis. Oncogene 2001;20:2401–12.
37. Burnstock G. The past, present and future of purine nucleotides as signalling molecules. Neuropharmacology 1997;36:1127–39.
38. Molliver DC, Cook SP, Carlsten JA, Wright DE, McCleskey EW. ATP and UTP excite sensory neurons and induce CREB phosphorylation through the metabotropic receptor, P2Y2. Eur J Neurosci 2002;16:1850–60.
39. Kawamura M, Terasaka O, Ebisawa T, Kondo I, Masaki E, Ahmed A, et al. Integrity of actin-network is involved in uridine 5′-triphosphate evoked store-operated Ca^{2+} entry in bovine adrenocortical fasciculata cells. J Pharmacol Sci 2003;91:23–33.
40. Naemsch LN, Weidema AF, Sims SM, Underhill TM, Dixon SJ. $P2X_4$ purinoceptors mediate an ATP-activated, non-selective cation current in rabbit osteoclasts. J Cell Sci 1999;112:4425–35.
41. Weidema AF, Dixon SJ, Sims SM. Activation of P2Y but not $P2X_4$ nucleotide receptors causes elevation of $[Ca^{2+}]_i$ in mammalian osteoclasts. Am J Physiol Cell Physiol 2001;280:C1531–9.
42. Furst DE, Saag K, Fleischmann MR, Sherrer Y, Block JA, Schnitzer T, et al. Efficacy of tacrolimus in rheumatoid arthritis patients who have been treated unsuccessfully with methotrexate: a six-month, double-blind, randomized, dose-ranging study. Arthritis Rheum 2002;46:2020–8.

A Splice Variant of the TCR ζ mRNA Lacking Exon 7 Leads to the Down-Regulation of TCR ζ, the TCR/CD3 Complex, and IL-2 Production in Systemic Lupus Erythematosus T Cells[1]

Kensei Tsuzaka,[2]*† Yumiko Setoyama,* Keiko Yoshimoto,* Kiyono Shiraishi,*† Katsuya Suzuki,*† Tohru Abe,* and Tsutomu Takeuchi*

The reduction or absence of TCR ζ-chain (ζ) expression in patients with systemic lupus erythematosus (SLE) is thought to be a factor in the pathogenesis of SLE. We previously reported a splice variant of ζ mRNA that lacks the 36-bp exon 7 (ζ mRNA/exon 7(−)) and is accompanied by the down-regulation of ζ protein in T cells from SLE patients. In this study, we show that EX7− mutants (MA5.8 cells deficient in ζ protein that have been transfected with ζ mRNA/exon 7(−)) exhibit a reduction in the expression of TCR/CD3 complex and ζ protein on their cell surface as well as a reduction in the production of IL-2 after stimulation with anti-CD3 Ab, compared with that in wild-type (WT) mutants (MA5.8 cells transfected with the WT ζ mRNA). Furthermore, real-time PCR analyses demonstrated that ζ mRNA/exon 7(−) in EX7− mutants was easily degraded compared with ζ mRNA by the WT mutants. Pulse-chase experiment showed ζ protein produced by this EX7− mutants was more rapidly decreased compared with the WT mutants. Thus, the lower stability of ζ mRNA/exon 7(−) might also be responsible for the reduced expression of the TCR/CD3 complex, including ζ protein, in SLE T cells. *The Journal of Immunology,* 2005, 174: 3518–3525.

Systemic lupus erythematosus (SLE)[3] is an autoimmune disease of unknown etiology (1–3). The disease is characterized by a large number of immunological abnormalities that appear to result from defects in T cells, B cells, and monocytes (4, 5). T cells are considered to be central to the pathogenesis of SLE because a dysfunction in their regulatory action may be responsible for the altered immune responses and overproduction of pathogenic autoantibodies (6). Abnormalities in peripheral blood T cells (PBTs) from SLE patients include T lymphocytopenia, low proliferative responses to lectin, anti-CD3 and anti-CD2 stimulation (7, 8), and a lower production of Th-1 type cytokines, such as IL-2 (9–11). Although the costimulatory pathway is up-regulated, the TCR/CD3 pathway appears to be down-regulated (12, 13). We and other groups have reported that a reduction in tyrosine phosphorylation and the diminished expression of TCR ζ protein (ζ) play crucial roles in the pathogenesis of SLE (14–16). Clinically, a reduction in ζ expression is not correlated with either the disease activity of SLE or the dose of prednisolone (17). In contrast, we and other groups have reported alterations in the ζ mRNA open reading frame (ORF) or the 3′-untranslated region of ζ mRNA in T cells from SLE patients (18–22). ζ has crucial roles in signal transduction through the TCR/CD3 complex (23–25) and in the efficient transport of the assembled TCR complexes to the cell surface (26). ζ is composed of three ITAM domains that are sufficient to couple chimeric receptors to early and late signaling events (24, 25, 27–32). The mutation of tyrosines within the ITAM or the nonphosphorylated and monophosphorylated motif abrogates the signal transduction ability (32, 33), suggesting that these tyrosines and their phosphorylation have crucial roles in protein function. Furthermore, ζ contains the GTP/GDP binding site, which is located immediately before the third ITAM (34). We have previously reported that 14 of 21 patients with SLE had decreased expression of ζ in PBTs. And 2 of the 14 SLE patients were lacking of the exon 7 portion of ζ mRNA (14). Exon 7 of ζ mRNA spans the GTP/GDP binding site proximal to the third ITAM. Thus, the aberrant ζ protein lacking exon 7 may result in skewed signal transduction, without efficient interaction with Shc and/or GTP/GDP. However, the involvement of ζ mRNA with an altered ORF, specifically in exon 7, in the decreased expression of ζ in SLE T cells has not been previously reported. To investigate the effect of ζ mRNA lacking exon 7 on the intracellular and cell surface expression of the ζ protein and TCR/CD3 complex, ζ cDNA lacking exon 7 (ζ cDNA/exon 7(−)) or wild-type (WT) ζ cDNA were transfected using a recombinant retrovirus system into murine T cell hybridomas (MA5.8) (35) deficient for ζ expression. In this study, we report that not only the expression of ζ protein, but also the expression of the TCR/CD3 complex, was down-regulated on the cell surface of the MA5.8 mutant cells expressing ζ mRNA/exon 7(−) because of a reduction in ζ mRNA stability.

Materials and Methods

Cell lines and inhibition of RNA synthesis

The MA5.8 cells (lacking endogenous ζ expression) were kindly provided by Prof. Takashi Saito (Chiba University, Chiba, Japan), and the RetroPackPT67 (BD Clontech) was used as the dualtropic packaging cell line.

*Second Department of Internal Medicine, Saitama Medical Center, Saitama Medical School, Kawagoe, Saitama, Japan; and †Research Center for Genomic Medicine, Saitama Medical School, Hidaka, Saitama, Japan

Received for publication February 27, 2004. Accepted for publication January 12, 2005.

The costs of publication of this article were defrayed in part by the payment of page charges. This article must therefore be hereby marked *advertisement* in accordance with 18 U.S.C. Section 1734 solely to indicate this fact.

[1] This work was supported by Grants-in-Aid for Scientific Research (C), the Ministry of Education, Science, and Culture, Japan.

[2] Address correspondence and reprint requests to Dr. Kensei Tsuzaka, Second Department of Internal Medicine, Saitama Medical Center, Saitama Medical School, Kamoda 1981, Kawagoe, Saitama 350-8550, Japan. E-mail address: kentsu@saitama-med.ac.jp

[3] Abbreviations used in this paper: SLE, systemic lupus erythematosus; Ct, threshold cycle; ER, endoplasmic reticulum; IP, immunoprecipitation; ORF, open reading frame; PBT, peripheral blood T cell; PVDF, polyvinylidene difluoride; WT, wild type; ζ, TCR ζ protein.

0022-1767/05/$02.00

For experiments involving the inhibition of RNA synthesis, cell cultures were incubated with 4 μg/ml actinomycin D in the culture medium. Samples were collected for up to 48 h after drug exposure.

DNA transfection and infection

The DNA transfection and infection protocols have been previously described (36). Full-length WT human ζ cDNA (ζ cDNA; +136~+1627 (1492 bp)) and human ζ cDNA lacking exon 7 (ζ cDNA/exon 7(−): +136~+564, +600~+1627 (1456 bp)) were amplified from the PBTs of a normal healthy control and an SLE patient (KS), respectively, using RT-PCR (Fig. 1). Each cDNA was ligated into a *Sal*I-cut pDON-AI (Takara Bio), and each of the pDON-AI construct was sequenced in both directions to verify the nucleotide sequences. Purified pDON-AI containing the WT ζ cDNA insert, the ζ cDNA/exon 7(−) insert, or without any DNA insert were then transfected into 5.0×10^6 RetroPackPT67 cells using a cationic liposome kit (TransFast Transfection Reagent; Promega). Forty-eight hours after transfection, 10 ml of DMEM was added to the cells, and supernatant containing the same amount of the vector retrovirus was subsequently used to infect 1.0×10^7 MA5.8 cells in the presence of 8 μg/ml polybrene. After 24 h of incubation, G418 was added to select the infected cells, and 30 random colonies were selected and cultured together to construct MA5.8 mutants (WT, EX7−, and NEG, respectively).

RT-PCR

Whole mRNA was isolated from the cell samples and the mRNA was converted to whole cDNA by reverse transcriptase, according to a previously described method (18). Using 5 μl of the whole cDNA as the template, specific cDNA was amplified by PCR using specific primers and TaqDNA polymerase (Applied Biosystems). The PCR conditions were as follows: denaturation at 95°C for 30 s, annealing at 55°C for 30 s, and extension at 72°C for 1 min, for a total of 35 cycles. The primers for amplifying the human full-length ζ cDNA were arranged upstream of the ORF 5′-TCAGCCTCTGCCTCCCAGCCTCTTTCT-3′ (+136 to +162) and 3′ end of exon 8 5′-GCAGAGCAGAGAGCGTTTTCCATCCAT-3′ (+1627 to +1601) of human ζ mRNA (37). To amplify the murine CD3ε cDNA (25), specific primers were arranged as follows: 5′-ATCCTGTGC CTCAGCCTCCTAGCTGT-3′ (+25 to +50) and 5′-ATGGGCTCAT AGTCTGGGTTGGGAA-3′ (+494 to +488). As a positive control, murine β-actin cDNA was amplified by PCR using the following primers: 5′-GGCCAACCGTGAAAAGATGA-3′ (+419 to +438) and 5′-CACGC TCGGTCAGGATCTTC-3′ (+669 to +650). PBTs were isolated from whole blood according to a previously described method (18).

Real-time PCR

The primers for human ζ were located in two different exons of each gene to avoid the amplification of any contaminating genomic DNA (37): the forward primer was 5′-TGCTGGATCCCAAACTCTGC-3′ (+254 to +272) (exon 3) and the reverse primer was 5′-CCCGGCCACGTC TCTTG-3′ (+434 to +449) (exon 5). The TaqMan probe was 5′-ATG GAATCCTCTTCATCTATGGTGTCATTCTCAC-3′ (+284 to +317) and had a fluorescent reporter dye (FAM) covalently linked to its 5′-end and a downstream quencher dye (TAMRA) linked to its 3′-end. The primers for murine CD3ε cDNA were located in two different exons of each gene (38): the forward primer was 5′-GGACAGTGGCTACTACGTCT GCTA-3′ (+307 to +330) (exon 4) and the reverse primer was 5′-TGAT GATTATGGCTACTGCTGTCA-3′ (+423 to +400) (exon 7). The TaqMan probe was 5′-CACCTCCACACAGTACTCACACACTCGA-3′ (+400 to +373). In addition, the forward primer of 5′-GGCCAACCGT GAAAAGATGA-3′ (+419 to +438) and the reverse primer of 5′-CACGCTCGGTCAGGATCTTC-3′ (+669 to +650) for the murine β-actin cDNA were designed in exon 3 and exon 4, respectively. The TaqMan probe for the murine β-actin cDNA was 5′-TTTGAGACCTTCAACAC CCCAGCCA-3′ (+450 to +474).

Amplification and detection of specific products were performed using an ABI PRISM 7700 sequence detection system (Applied Biosystems) according to a previously described amplification protocol (36). To prepare a template DNA standard, a target DNA fragment was amplified by PCR and was fused into pCRII vector by using TA cloning kit (Invitrogen Life Technologies), amplified, and refined. The amount of standard DNA construct per well was adjusted to 10 pg and then serially diluted, yielding samples containing 10, 1, 10^{-1}, 10^{-2}, and 10^{-3} pg, which were then used to construct standard plots.

Cell surface biotinylation, immunoprecipitation (IP), and SDS-PAGE

Cells (1.0×10^7 cells/ml) were biotinylated in bicarbonate buffer to label the cell surface proteins using a previously described method (36). Cells were then lysed, and the cleared lysates were immunoprecipitated for 2 h at 4°C with 2 μg of mouse anti-human ζ mAb (TIA-2) (Coulter Immunology), rabbit anti-mouse TCRα mAb (Santa Cruz Biotechnology), rabbit anti-mouse TCRβ mAb (Santa Cruz Biotechnology), goat anti-mouse CD3ε mAb (Santa Cruz Biotechnology), goat anti-mouse CD3γ mAb (Santa Cruz Biotechnology), or goat anti-mouse CD3δ mAb (Santa Cruz Biotechnology) bound to 15 μl of equilibrated protein G-Sepharose (Amersham Biosciences). The resulting pellets were resuspended in a nonreducing sample buffer and loaded on a 12% SDS-PAGE.

Western blot analysis

Cells were lysed with the lysis buffer and disrupted by sonication according to a previously described method (17). After centrifuging at 10,000 × *g* for 5 min, the supernatant was loaded on a 15% SDS-PAGE gel using a reducing method. The proteins were electrophoretically blotted onto polyvinylidene difluoride (PVDF) membranes (Millipore), and the membranes were soaked at 37°C for 1 h in blocking agents (Blockace; Dainippon Pharmaceuticals). The blots were then probed with a mouse anti-human ζ mAb (TIA-2) at 16°C for 1 h. TIA-2 was visualized using a peroxidase-conjugated anti-mouse IgG (Amersham Biosciences). Biotinylated proteins were detected using streptavidin-peroxidase (Southern Biotechnology Associates). After washing three times, the signals were detected by chemiluminescence-enhancing reagents (Amersham Biosciences). The treated membranes were visualized on ECL x-ray film (Amersham Biosciences). The density of the specific bands was quantified as index by scanning with a Scan Jet II (Hewlett Packard) and National Institutes of Health Image Software (version 1.56).

Flow cytometric analysis

The flow cytometric analysis procedure has been previously described (17). Briefly, MA5.8 or the transfectants were stained with a FITC-conjugated Armenian hamster anti-mouse CD3ε mAb (145-2C11) (Coulter Immunology) or an FITC-conjugated mouse anti-human ζ mAb (TIA-2) (Coulter Immunology). The analysis was performed using a FACScan flow cytometer and consort-30 software. An FITC-conjugated Armenian hamster anti-mouse IgG (Coulter Immunology) and an FITC-conjugated mouse anti-human IgG (Coulter Immunology) were used as negative controls.

Pulse-chase experiment

Cells (3.0×10^7) were collected and washed twice with PBS. Cells were labeled in methionine-free RPMI 1640 medium (Sigma-Aldrich) containing 0.21 mCi of ProMix [^{35}S]methionine in vitro cell labeling mix (Amersham Biosciences). Five hours later, the medium was removed, cells were washed three times with PBS and were chased with RPMI 1640 medium containing methionine for 0, 2, and 4 h. Cells were then washed three times with PBS and incubated for 15 min with 200 μl of lysis buffer. The cell lysates were centrifuged at 10,000 × *g* for 5 min. The supernatant was retained for protein assay using the BCA protein kit (Pierce). Equal amounts of proteins for each condition were then immunoprecipitated. Protein bands were detected by autoradiography using BAS5000 system (Fuji Photo Film).

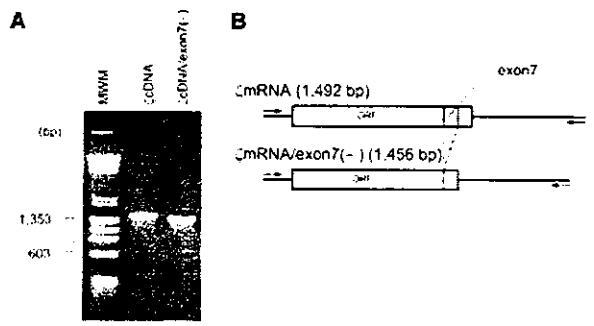

FIGURE 1. RT-PCR of human ζ cDNA lacking exon 7. *A*, WT human full-length ζ cDNA (ζ cDNA) (1492 bp) and human ζ cDNA lacking exon 7 (ζ cDNA/exon 7(−)) (1456 bp) were amplified by RT-PCR from PBTs obtained from a healthy normal control and an SLE patient (KS), respectively, and electrophoresed on an agarose gel (1.0%). *B*, ζ mRNA/exon 7(−) is lacking the 36-bp region corresponding to exon 7. The arrows indicate the specific primers used to amplify the full-length ζ cDNA.

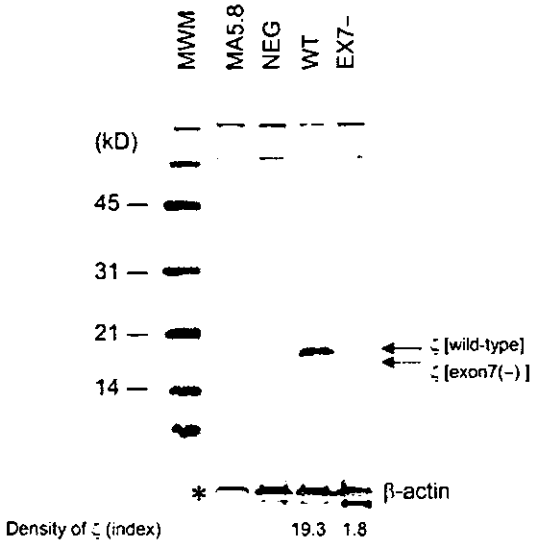

FIGURE 2. Western blot analysis of human ζ expressed by MA5.8 mutants. Cell lysates from MA5.8 and its mutants (NEG, WT, and EX7−) were electrophoresed on 15% SDS-polyacrylamide gels using a reducing method and blotted onto a PVDF membrane. The membranes were then incubated with a mouse anti-human ζ mAb (TIA-2) followed by a peroxidase-conjugated anti-mouse IgG. After treatment with chemiluminescence-enhancing reagents, the membranes were visualized on ECL x-ray films, and the densities of the 18-kDa WT ζ protein (ζ[wild-type]) and the 17-kDa short-form exon 7-deleted ζ protein (ζ[exon 7(−)]) bands (indicated by the arrows) were quantified as index. *, Western blot of the MA5.8 mutants using a hamster anti-mouse β-actin mAb.

Intracellular staining for ζ, CD3ε, and endoplasmic reticulum (ER)

Cells were resuspended in PBS, laid on poly-L-lysine-coated slides for 15 min at 37°C, and fixed for 10 min with 4% paraformaldehyde, and permeabilized for 10 min at room temperature with washing buffer (HEPES-buffered PBS containing 0.1% Triton X-100). Cells were then stained with FITC-conjugated Armenian hamster anti-mouse CD3ε mAb (145-2C11) (BD Pharmingen) in PBS containing 1% BSA, a mouse anti-human ζ mAb (6B10.2) (Santa Cruz Biotechnology), followed by Alexa Fluor 568 goat anti-mouse IgG (H+L) (Molecular Probes), and a rabbit polyclonal Ab to calreticulin (Novus Biologicals) followed by Alexa Fluor 647 $F(ab')_2$ of goat anti-rabbit IgG (H+L) (Molecular Probes). The samples were mounted in DakoCytomation Fluorescent Mounting Medium (DakoCytomation) and were examined using a Leica TCS SP2 confocal microscope (Leica Camera).

Ab stimulation and IL-2 quantification

Anti-mouse CD3 mAb (KT3) (Coulter Immunology) was bound for 16 h to a 24-well, flat-bottom plate in PBS. The wells were rinsed with fresh PBS three times before the addition of the cells. Fifty microliters of transfected cells (1.0×10^6 cells/ml) were added to each well and incubated at 37°C in 7.0% CO_2. Culture supernatants were harvested, and their aliquots were collected and frozen at 1, 2, and 3 days after stimulation. The harvested supernatants were assayed using a standard IL-2 assay. Recombinant murine IL-2 (BD Pharmingen) was used as a standard.

Statistical analysis

Statistical significance was calculated using the Student's t test for unpaired data using Statview software (version 4.5; Abacus). A value of $p < 0.05$ was considered statistically significant.

Results

Western blot analysis of ζ protein in MA5.8 mutants expressing ζ mRNA/exon 7(−)

In a Western blot analysis using an anti-human ζ mAb (TIA-2), the production of the exon 7-deleted ζ (16 kDa) by the EX7− mutants was only 9.3% (index ratio, 1.8:19.3) of the WT ζ (18 kDa) produced by the WT mutants (Fig. 2). Therefore, we concluded that the expression of ζ protein was reduced in mutants containing ζ mRNA/exon 7(−).

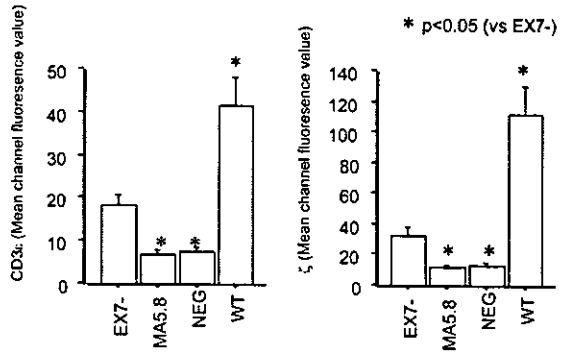

FIGURE 3. Flow cytometric analysis of the MA5.8 mutants. The surface expression of the TCR/CD3 complex and the ζ protein on MA5.8 and its mutants (NEG, WT, and EX7−) was quantified as the mean channel fluorescence value using FITC-conjugated anti-mouse CD3ε mAb (145-2C11) and FITC-conjugated anti-human ζ mAb (TIA-2), respectively. Each experiment was performed in triplicate. The mean channel fluorescence value of the EX7− mutants was compared with that of MA5.8 and the other MA5.8 mutants (MA5.8, NEG, and WT), respectively. Statistical significance was calculated using Student's t test. Bars show the mean ± SD.

Analysis of ζ protein and TCR/CD3 complex on the cell surface of MA5.8 mutants expressing ζ mRNA/exon 7(−) by FACS and IP

To investigate the expression of ζ protein and the TCR/CD3 complex on the cell surface, MA5.8 and its mutants were stained with an FITC-conjugated anti-mouse CD3ε mAb (145-2C11) or an FITC-conjugated anti-human ζ mAb (TIA-2) and analyzed by flow cytometry (Fig. 3). This experiment was performed in triplicate. Although the expression of ζ protein on the cell surface of EX7− mutants (mean channel fluorescence value, 34.48 ± 5.07 (mean ± SD)) was significantly ($p < 0.05$) up-regulated, compared with the MA5.8 cells (12.52 ± 1.50) and the NEG (13.78 ± 1.58) mutants, it was significantly ($p < 0.05$) lower than that of the WT mutants (112.19 ± 18.27). The CD3ε expression level on the EX7− mutants (18.44 ± 2.50) was significantly ($p < 0.05$) higher than those on the MA5.8 cells (7.00 ± 1.00) and the NEG mutants (7.49 ± 1.25). However, it was significantly ($p < 0.05$) lower than that on the WT mutants (41.74 ± 6.51).

To confirm the cell surface expression of ζ protein and the TCR/CD3 complex, we subjected MA5.8 and its mutants to surface biotinylation, IP, SDS-PAGE analysis under nonreducing conditions, and Western blot analysis (Fig. 4). IP of the WT mutants with both hamster anti-mouse CD3ε mAb (145-2C11) and mouse anti-human ζ mAb (TIA-2) yielded the following surface labeled proteins: mature forms of the TCR$\alpha\beta$ heterodimers ($\alpha\beta_m$) (67–95 kDa), a ζ homodimer (34 kDa) (indicated as the open arrowheads), CD3γ (26 kDa), CD3δ (28 kDa), and CD3ε (23 kDa), indicating that TCR/CD3 complex is producing on the WT mutants. The protein bands of the TCR/CD3 components were confirmed by the Western blot and IP of a whole cell lysate of the WT mutants with Abs against each TCR/CD3 component. IP of the WT mutants with nonspecific hamster and mouse IgG did not yield any of these proteins (data not shown). Interestingly, IP of the EX7− mutants with anti-CD3ε mAb or anti-human ζ mAb demonstrated a reduced expression of the cell surface short ζ homodimer (32 kDa) (indicated as the closed arrowheads) as well as a decreased expression of the cell surface CD3γ and CD3ε accompanied with the absence of CD3δ, indicating the down-regulation of TCR/CD3 complex on the cell surface of EX7− mutants.

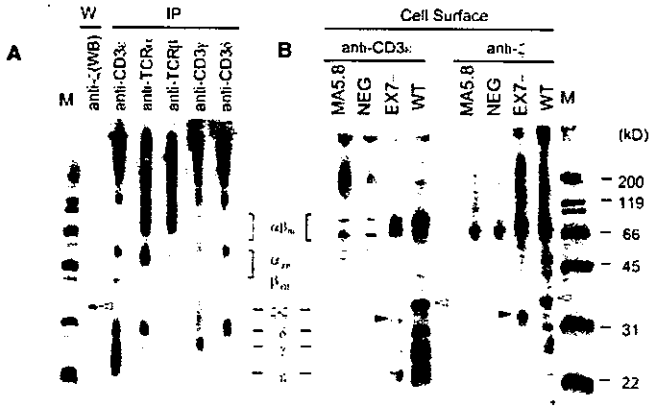

FIGURE 4. *A*, Western blot and IP of TCR/CD3 components in WT mutant. The cell lysates from WT mutants were electrophoresed on 12% SDS-polyacrylamide gels using a nonreducing method and were blotted onto a PVDF membrane. The membranes were then incubated with a mouse anti-human ζ mAb (TIA-2) followed by a peroxidase-conjugated anti-mouse IgG (*lane W*). The cell lysates from WT were immunoprecipitated using a goat anti-mouse CD3ε mAb (145-2C11), rabbit anti-mouse TCRα and TCRβ mAbs, and goat anti-mouse CD3γ and CD3δ mAbs bound to protein G-Sepharose. The pellets were electrophoresed on 12% SDS-polyacrylamide gels using a nonreducing method and were blotted onto a PVDF membrane. The membranes were then incubated with the Ab against each TCR/CD3 component, followed by a peroxidase-conjugated anti-goat or anti-rabbit IgG (*lane IP*). $\alpha\beta_m$, α_{im}, and β_{im} indicate the mature forms of the TCR αβ-chains, the immature forms of TCRα, and the immature forms of the TCR β-chains, respectively. *B*, IP of cell surface TCR/CD3 complexes and ζ protein in MA5.8 and its mutants. MA5.8 and its mutants (NEG, EX7−, and WT) were biotinylated and lysed in a cell lysis buffer. The cell lysates were immunoprecipitated using goat anti-mouse CD3ε mAb (145-2C11) or mouse anti-human ζ mAb (TIA-2) bound to protein G-Sepharose. The pellets were resuspended in a nonreducing sample buffer and loaded on a 12% SDS-PAGE. Biotinylated proteins were blotted onto PVDF membranes and detected using streptavidin-peroxidase. After treatment with chemiluminescence-enhancing reagents, the membranes were visualized on ECL x-ray films. M, The protein molecular markers. The open and closed arrowheads indicate the protein bands of the WT (34-kDa) and the exon 7-deleted short-form (32-kDa) ζ homodimer, respectively.

Confocal microscopic analysis of MA5.8 cells

To explore the intracellular localization of TCR/CD3 complex including ζ in the MA5.8 mutants, WT and EX7− mutants were fixed, permeabilized, and stained with anti-ζ, anti-CD3ε, and anti-calreticulin Abs, respectively (Fig. 5). The staining of the WT mutant with 6B10.2 (anti-ζ, red in Fig. 5) and 145-2C11 (anti-CD3ε, green in Fig. 5) observed in a confocal microscopy showed the ring-shaped pattern (indicated as the white arrows), indicating the cell surface expression of TCR/CD3 complex including ζ in the WT mutants. In contrast, the staining pattern of the EX7− mutants with 6B10.2 (anti-ζ) or 145-2C11 (anti-CD3ε) was similar to that with anti-calreticulin Ab (indicated as the yellow arrows), indicating the staining of the ER detected by anti-calreticulin (blue in Fig. 5) as well as some weak dots on the cell surface (indicated as the yellow arrow), indicating low expression of the original TCR/CD3 complex of MA5.8 cells. From these observations, most of the TCR/CD3 complex in the EX7− mutants could be retained in the ER.

Decrease in IL-2 production in MA5.8 mutants expressing ζ mRNA/exon 7(−)

To evaluate the effect of exon 7 deletion in ζ mRNA, MA5.8 mutants were stimulated with anti-mouse CD3ε mAb (145-2C11)

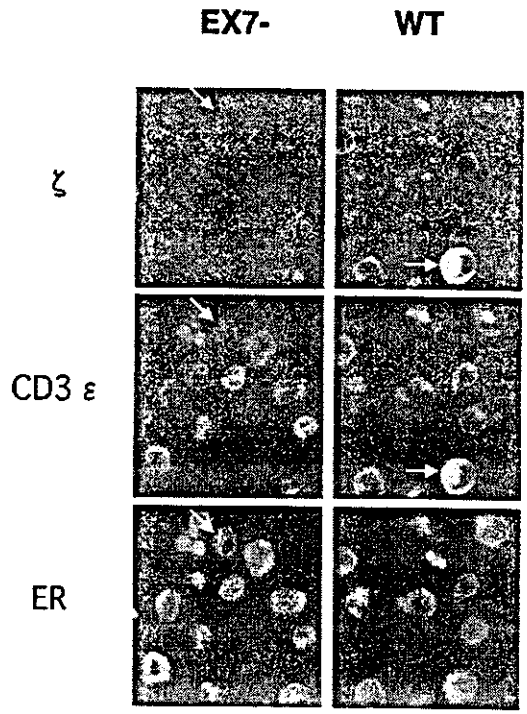

FIGURE 5. Intracellular staining for ζ, CD3ε, and ER. The EX7− and WT mutants were laid on poly-L-lysine-coated slides, fixed with 4% paraformaldehyde, and permeabilized with washing buffer. Cells were then stained with FITC-conjugated Armenian hamster anti-mouse CD3ε mAb (145-2C11) (green color), a mouse anti-human ζ mAb (6B10.2), followed by Alexa Fluor 568 goat anti-mouse IgG (H+L) (red color), and a rabbit polyclonal Ab to calreticulin followed by Alexa Fluor 647 $F(ab')_2$ of goat anti-rabbit IgG (H+L) (blue color). The samples were mounted and were examined using a confocal microscope. White arrows show the ring-shaped pattern of the WT mutants with 6B10.2 and 145-2C11, whereas yellow arrows indicate the cytoplasmic pattern of the EX7− mutants with 6B10.2, 145-2C11, and anti-calreticulin Ab.

(Fig. 6). IL-2 production in the WT, NEG, or MA5.8 mutants on day 1, 2, or 3 after stimulation was compared statistically with that in the EX7− mutants. IL-2 production in the EX7− mutants on day 1 (1.50 ± 2.12 ng/ml), day 2 (3.00 ± 4.24 ng/ml), and day 3 (4.50 ± 0.71 ng/ml) was significantly ($p < 0.01$) lower than that in the WT mutants on day 1 (54.00 ± 0.00 ng/ml), day 2 (81.50 ± 3.54 ng/ml), and day 3 (89.50 ± 2.12 ng/ml), respectively. Consequently, IL-2 production in the MA5.8 mutants expressing ζ mRNA/exon 7(−) was lower than that in the MA5.8 mutants expressing WT ζ mRNA.

ζ mRNA stability assay

To evaluate the relationship between the reduction in ζ protein expression and exon 7 deletion, we examined the stability of ζ mRNA. WT and EX7− mutants were exposed to actinomycin D to inhibit transcription. The cell cultures were incubated with 4 μg/ml actinomycin D, and the cells were collected at 0, 6, 12, 24, and 48 h after drug exposure. One microgram of whole mRNA was isolated from the cell samples and converted to whole cDNA by reverse transcriptase. Using 5 μl of the whole cDNA as the template, ζ, CD3ε, and β-actin cDNA in the WT or the EX7− mutants were quantified by real-time PCR. To validate the real-time PCR, the standard curves for human ζ, murine CD3ε, and murine β-actin gene were constructed from the pCRII fused with ζ cDNA (1492 bp), CD3ε cDNA (470 bp), and β-actin cDNA (250 bp), respectively. The critical threshold cycle (Ct) for ζ, CD3ε, and β-actin cDNA was inversely proportional (correlation coefficient of all

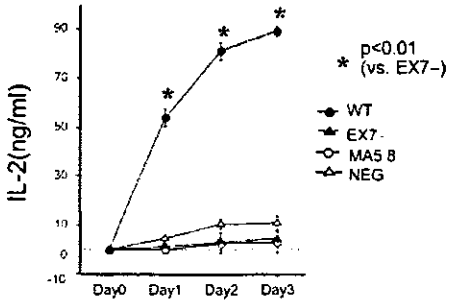

FIGURE 6. IL-2 production in MA5.8 mutants after stimulation with anti-CD3ε Ab. Anti-mouse CD3ε mAb (145-2C11) was bound to a 96-well, flat-bottom plate. MA5.8 and its mutants (NEG, WT, and EX7−) were then added to the wells and incubated. The culture supernatants were collected 1, 2, and 3 days after stimulation and assayed using a standard IL-2 assay. Each experiment was performed in triplicate. IL-2 production in WT, NEG, or MA5.8 on day 1, 2, or 3 after stimulation was compared statistically with that in EX7− mutants by using Student's *t* test. Bars show the mean ± SD.

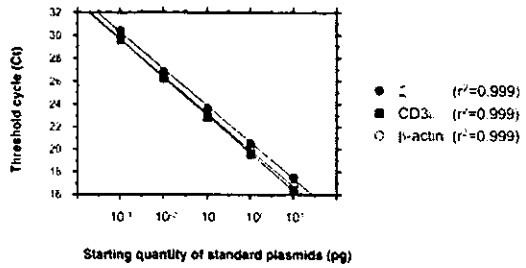

FIGURE 7. Standard curves for quantifying the amount for ζ, CD3ε, and β-actin cDNA. Human ζ ORF cDNA (1492 bp), murine CD3ε cDNA (470 bp), and murine β-actin cDNA (250 bp) were fused with pCRII vector, respectively. Real-time PCR was performed with the serial dilution (10, 1, 10^{-1}, 10^{-2}, and 10^{-3} pg) of the plasmid DNA as the template to estimate the critical Ct.

three genes was 0.999) to the logarithm of the initial amount of the standard template DNA (Fig. 7). Then the Ct for these cDNA were measured by the real-time PCR. These cDNA were measured by three separate experiments, and the statistical significance was calculated using the Student's *t* test. As a result, demonstrated in Table I and Fig. 8*A*, the transcript of CD3ε and β-actin in the two MA5.8 mutants was gradually degraded over time after the treatment of actinomycin D. Decrease in the expression of these mRNA itself was not affected following the transfection of ζ mRNA because there was no observed difference in the protein expression of ζ and CD3ε of the WT or EX7− mutants at 0, 24, and 48 h after the transfection by Western blot (data not shown). However, there seemed to be a difference in the kinetics of mRNA stability between the WT and EX7− mutants because the transcripts of β-actin in the WT mutants were easily degraded compared with the EX7− mutants at 6 h after the actinomycin D treatment. The amount of ζ or CD3ε transcript was evaluated as the relative quantity against β-actin cDNA (Table I and Fig. 8*B*). As a result, the relative amount of ζ mRNA in the EX7− mutants (0.008 ± 0.001) was already significantly ($p < 0.01$) lower than that in the WT mutants (0.014 ± 0.002) before the actinomycin D treatment. And the relative amount of the WT ζ mRNA in the WT mutants increased constantly, while that of the ζ mRNA/exon 7(−) in the EX7− mutants did not change and was significantly ($p < 0.01$) lower than that of the WT ζ transcript over time (Fig. 8*Bi*). In contrast, relative amount of CD3ε mRNA in both MA5.8 mutants was almost the same at 0, 12, and 48 h after the actinomycin D treatment. From these observations, we can conclude that the ζ mRNA/exon 7(−) in the EX7− mutants was less stable than the WT ζ mRNA in the WT mutants. In contrast, the stability of the CD3ε mRNA was similar in the EX7− mutants and the WT mutants (Fig. 8*Bii*).

Pulse-chase experiment using MA5.8 mutants

To confirm whether decreased stability of the ζ mRNA/exon 7(−) in the EX7− mutants could be related to the reduced amount of ζ protein, we compared the production of ζ in the WT and EX7− mutants. After labeling with [^{35}S]methionine in methionine-free medium for 5 h, WT and EX7− mutants were chased with the complete medium for 0, 2, and 4 h. The cell lysate was then incubated with mouse anti-human ζ mAb (TIA-2) bound to protein G-Sepharose. The resulting pellets were resuspended in a nonreducing sample buffer and loaded on a 12% SDS-PAGE followed by the autoradiography. As shown in Fig. 9, short ζ homodimer (32 kDa) produced by the EX7− mutants (indicated as the closed arrowheads) was gradually decreased over time, whereas the expression level of the WT ζ homodimer (34 kDa) produced by the WT mutants (indicated as the open arrowheads) did not change even after 4 h from chasing. From these observations, reduced ζ mRNA/exon 7(−) due to altered transcription and/or mRNA stability could lead to decreased ζ protein formation; as degradation of mRNA occurs, less protein is made.

Table I. *mRNA stability assay for the EX7− or WT mutants*

		0 h	6 h	12 h	24 h	48 h
Amount of cDNA (× 0.01 pg)						
EX7−	ζ	0.605 ± 0.058	0.789 ± 0.291	1.068 ± 0.197	0.471 ± 0.064	0.303 ± 0.052
	CD3ε	3.190 ± 0.356	5.549 ± 0.242	3.778 ± 0.503	0.608 ± 0.023	0.059 ± 0.008
	β-actin	73.292 ± 1.100	85.049 ± 2.462	34.860 ± 2.886	5.103 ± 0.097	1.431 ± 0.190
WT	ζ	1.970 ± 0.243	1.712 ± 0.169	1.067 ± 0.232	0.613 ± 0.026	0.286 ± 0.049
	CD3ε	7.319 ± 0.505	0.997 ± 0.034	0.132 ± 0.004	0.024 ± 0.003	0.005 ± 0.001
	β-actin	138.530 ± 5.495	12.063 ± 0.517	2.138 ± 0.053	0.514 ± 0.041	0.133 ± 0.019
Relative amount of cDNA						
ζ:β-actin ratio	EX7−	0.008 ± 0.001	0.009 ± 0.003	0.031 ± 0.006	0.092 ± 0.013	0.212 ± 0.036
	WT	0.014 ± 0.002 *	0.142 ± 0.014 **	0.499 ± 0.108 **	1.193 ± 0.051 *	2.152 ± 0.365 **
CD3ε:β-actin ratio	EX7−	0.044 ± 0.005	0.065 ± 0.003	0.108 ± 0.014	0.119 ± 0.005	0.041 ± 0.005
	WT	0.053 ± 0.004 N.S.	0.082 ± 0.003 **	0.061 ± 0.002 N.S.	0.047 ± 0.005 *	0.034 ± 0.005 N.S.

*, $p < 0.01$.
**, $p < 0.001$.

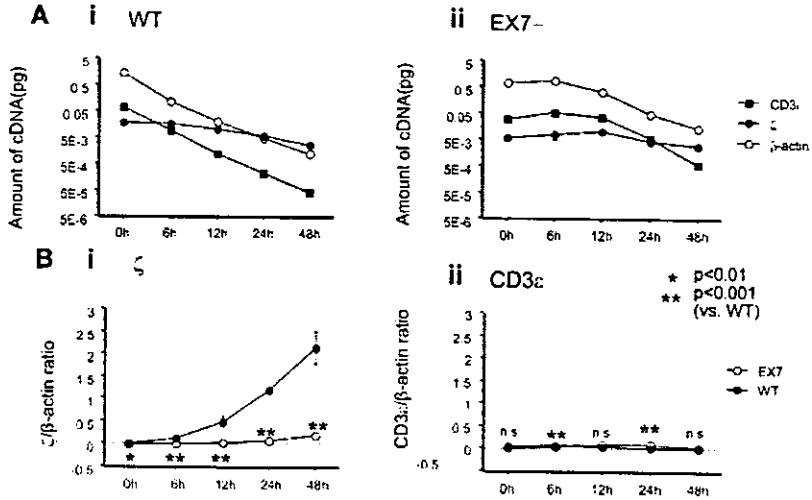

FIGURE 8. Reduction in ζ mRNA stability in the absence of the 36-bp portion of exon 7. MA5.8 mutants (WT and EX7−) were cultured and incubated with 4 μg/ml actinomycin D in the culture medium. Samples were collected at various time points, and the mRNA was subsequently extracted and converted to whole cDNA. *A*, Using 5 μl of the whole cDNA as the template, ζ, CD3ϵ, and β-actin cDNA in the WT (*i*) or the EX7− mutants (*ii*) were quantified by real-time PCR. Each experiment was performed in triplicate. *B*, The amount of ζ (*i*) or CD3ϵ (*ii*) mRNA expression was evaluated as the relative quantity against β-actin cDNA in WT (●) or EX7− mutants (○). Bars show the mean ± SD. *, $p < 0.01$; **, $p < 0.001$ of EX7− vs WT.

Discussion

We previously reported that ζ mRNA/exon 7(−), a splice variant of ζ mRNA, was detected in SLE T cells (14). The cytoplasmic domain of ζ is sufficient for coupling to receptor-associated signal transduction (25). This cytoplasmic domain contains three ITAM domains that, when phosphorylated, serve as docking sites for signaling proteins like ZAP70, actin, PI3K, and Shc. In particular, PI3K preferentially binds to ITAM1 (39), whereas Shc and the actin cytoskeleton interact predominantly with ITAM3 (40, 41). The ITAM sequence alone is sufficient to couple chimeric receptors to early and late signaling events (27). Mutations at tyrosines within the ITAM or nonphosphorylated and monophosphorylated motifs abrogate the signal transduction ability (32), suggesting a crucial role for phosphorylation of tyrosines. The GTP/GDP binding site, a glycine-rich sequence of GxxxxGKGxxGxxxG, is a unique portion that has the capacity to bind GTP/GDP, but not GMP or ATP, and is responsible for the G protein signaling pathway (38). The ζ mRNA mutation of the exon 7 deletion found in SLE patients influenced the ITAM3 domain and the GTP/GDP binding site, two regions that are critical for signal transduction involving the ζ protein. In this study, we attempted to confirm that a reduction in ζ protein expression occurs in cells containing ζ mRNA/exon 7(−) using a recombinant retrovirus system described by Bolliger et al. (42) and Weissman et al. (43).

The down-regulation and smaller size of the ζ protein in EX7−, as confirmed by the Western blot analysis, suggests that the production of the smaller ζ protein is down-regulated when it is translated from ζ mRNA/exon 7(−) because of the exon 7 deletion. These observations were also confirmed by IP and FACS analyses. Reportedly, TCR/CD3 complexes cannot be expressed on the cell surface without binding to the ζ homodimer in the cytoplasm (44–46). Therefore, in the MA5.8 mutants expressing ζ mRNA/exon 7(−), the TCR/CD3 complex might be down-regulated on the cell surface because of the reduction in the expression of ζ homodimer in IP using biotinylated cell surface proteins. Confocal microscopic analysis also revealed reduced cell surface expression of the ζ protein and the retention of TCR/CD3 complex in the cytoplasm of the EX7− mutant. Other groups have shown that the expression of the detergent-insoluble membrane-associated form of ζ was reduced in SLE T cells (47), supporting our results. The reduction in IL-2 production in the EX7− mutants revealed that the signal from the TCR was not transduced into the cytoplasm by anti-CD3ϵ Ab stimulation in this MA5.8 mutant. The results obtained using the MA5.8 mutants in this study may explain the mechanism behind the reduction in ζ protein expression in SLE T cells.

We examined the stability of ζ mRNA to investigate the reduction in ζ protein expression in the MA5.8 mutants expressing ζ mRNA/exon 7(−). From our observations, ζ mRNA/exon 7(−) in the EX7− mutants appeared to be less stable and more easily degraded than the WT ζ mRNA in the WT mutants. In pulse-chase experiment, ζ protein produced by the EX7− mutants was gradually decreased while the expression level of the ζ protein by the WT mutants did not change over time. From these observations, unstable ζ mRNA/exon 7(−) in the EX7− mutants could be related to the reduced amount of ζ protein. Therefore, it is conceivable that a reduction in ζ mRNA/exon 7(−) stability may lead to a reduction in the expression of ζ homodimer, leading to the absence of TCR/CD3 complex expression on the cell surface. The lower basal levels of ζ mRNA/exon 7(−) that were observed in the EX7− mutants before the treatment of actinomycin D, compared with that of the WT ζ mRNA in WT, may also be caused by mRNA instability in the EX7− mutants. Moreover, other reasons for reduced protein including increased degradation by a ubiquitin-proteasome pathway, as shown by Tsokos and colleagues (47), could also contribute to decrease expression of ζ in SLE T cells.

Several reports have been made on the relationship between exon deletion or exon skipping and the down-regulation of protein expression. Leitner et al. (48) reported that exon 3 skipping in (6*R*)-5,6,7,8-tetrahydro-L-biopterin mRNA in human monocytes/macrophages leads to the down-regulation of protein synthesis.

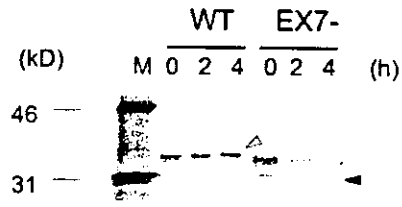

FIGURE 9. Pulse-chase experiment of MA5.8 mutants. A total of 3.0×10^7 of MA5.8 mutants (WT and EX7−) was collected and washed twice with PBS. Cells were labeled in methionine-free RPMI 1640 medium containing ProMix [^{35}S]methionine in vitro cell labeling mix. Five hours later, the medium was removed, and cells were chased with RPMI 1640 medium containing methionine for 0, 2, and 4 h. Cells were then washed with PBS and incubated for 15 min with lysis buffer. The cell lysate was then incubated with mouse anti-human ζ mAb (TIA-2) bound to protein G-Sepharose. The resulting pellets were resuspended in a nonreducing sample buffer and loaded on a 12% SDS-PAGE. Protein bands were detected by autoradiography using BAS5000 system. M, The protein molecular markers of ^{14}C-methylated proteins.

Krummheuer et al. (49) also demonstrated that an alternative splicing pattern in HIV type 1 mRNA, resulting in the production of exon 2 as the leader exon, stimulates protein synthesis in HIV type 1 viruses. Exon-deletion or exon-skipping in mRNA has also been reported to be correlated with mRNA instability. Schwarze et al. (50) reported that frameshift mutations producing a premature termination codon in exon 6, 9, or 27 of type III procollagen mRNA leads to a reduction in both mRNA stability and protein synthesis. Kawamoto (51) demonstrated that the nucleotide region from +62 to +166, representing exon 1, of the nonmuscle myosin H chain-A gene could up-regulate its protein synthesis by affecting the pretranslational steps (transcriptional and mRNA stability). In contrast, parathyroid hormone-related protein mRNA containing exon 7 and exon 8 was reported to be stable, whereas that including exon 9 was unstable (52). From our observations in the present study, the deleted 36-bp portion representing exon 7 in ζ mRNA appears to be critical for ζ mRNA stability and may be correlated with the down-regulation of ζ and the TCR/CD3 complex in SLE T cells. Actually, cell surface expression of TCR/CD3 complex including ζ was reduced in T cells of the two SLE patients (patients HE and KS), who were lacking of exon 7 portion in their ζ mRNA (14). As we have found ζ mRNA/exon 7(−) in only 2 of 21 lupus patients, it will be important to determine how frequent this mutation occurs in the T cells of a large population and how it contributes to abnormal T cell functions, such as cytotoxicity. Previously, we reported that the expressions of ζ and the TCR/CD3 complex were down-regulated on the cell surface of MA5.8 mutant cells expressing ζ mRNA containing an alternatively spliced 3′-untranslated region because of a reduction in ζ mRNA stability (36). SLE T cells bear both the WT and the splice variant of ζ mRNA (22). Thus, it would be interesting to compare the combined effect of transfection of both WT and the splice variant form of ζ mRNA on IL-2 production and cell surface expression of TCR/CD3 complex to explore whether these splice variants of ζ mRNA are more dominant. This project is now underway in our laboratory. Taken together, the reduced stability of ζ mRNA produced by aberrant ζ mRNA forms might be crucial to explaining the reduced expression of ζ seen in SLE T cells.

Acknowledgments

We thank Prof. Takashi Saito (Chiba University) for providing the MA5.8 cells.

Disclosures

The authors have no financial conflict of interest.

References

1. Boumpas, D. T., H. A. R. Austin, B. J. Fessler, J. E. Balow, J. H. Klippel, and M. D. Lockshin. 1995. Systemic lupus erythematosus: emerging concepts. Part 1: renal, neuropsychiatric, cardiovascular, pulmonary, and hematologic disease. *Ann. Intern. Med. 122:940.*
2. Boumpas, D. T., B. J. Fessler, H. A. r. Austin, J. E. Balow, J. H. Klippel, and M. D. Lockshin. 1995. Systemic lupus erythematosus: emerging concepts. Part 2: dermatologic and joint disease, the antiphospholipid antibody syndrome, pregnancy and hormonal therapy, morbidity and mortality, and pathogenesis. *Ann. Intern. Med. 123:42.*
3. Mills, J. A. 1994. Systemic lupus erythematosus. *N. Engl. J. Med. 30:1871.*
4. Cohen, P. L. T- and B-cell abnormalities in systemic lupus. 1993. *J. Invest. Dermatol. 100:69s.*
5. Tsokos, G. C. Lymphocyte abnormalities in human lupus. 1992. *Clin. Immunol. Immunopathol. 63:7.*
6. Kotzin, B. L. 1996. Systemic lupus erythematosus. *Cell 85:303.*
7. Gottlieb, A. B., R. G. Lahita, N. Chiorazzi, and H. G. Kunkel. 1979. Immune function in systemic lupus erythematosus: impairment of in vitro T cell proliferation and in vivo antibody response to exogenous antigen. *J. Clin. Invest. 63:885.*
8. Fox, D. A., J. A. Millard, J. Treisman, W. Zeldes, A. Bergman, J. Depper, R. Dunne, and W. J. McCune. 1991. Defective CD2 pathway T cell activation in systemic lupus erythematosus. *Arthritis Rheum. 34:561.*
9. Huang, Y. P., P. A. Miescher, and R. H. Zubler. 1986. The interleukin 2 secretion defect in vitro in systemic lupus erythematosus is reversible in rested cultured T cells. *J. Immunol. 137:3515.*
10. Linker-Israeli, M. 1992. Cytokine abnormalities in human lupus. *Clin. Immunol. Immunopathol. 63:10.*
11. Horwitz, D. A., J. D. Gray, S. C. Behrendsen, M. Kubin, M. Rengaraju, K. Ohtsuka, and G. Trinchieri. 1998. Decreased production of interleukin-12 and other Th1-type cytokines in patients with recent-onset systemic lupus erythematosus. *Arthritis Rheum. 41:838.*
12. Stohl, W., J. E. Elliot, L. Li, E. R. Podack, D. H. Lynch, and C. O. Jacob. 1997. Impaired nonrestricted cytolytic activity in systemic lupus erythematosus. *Arthritis Rheum. 40:1130.*
13. Takeuchi, T., S. Tanaka, A. D. Steinberg, M. Matsuyama, J. Daley, S. F. Schlossman, and C. Morimoto. 1988. Defective expression of the 2H4 molecule after autologous mixed lymphocyte activation in systemic lupus erythematosus patients. *J. Clin. Invest. 82:1288.*
14. Takeuchi, T., K. Tsuzaka, M. Pang, K. Amano, J. Koide, and T. Abe. 1998. TCRζ chain lacking exon 7 in two patients with systemic lupus erythematosus. *Int. Imunnol. 10:911.*
15. Liossis, S. N., X. Z. Ding, G. J. Dennis, and G. C. Tsokos. 1998. Altered pattern of TCR/CD3-mediated protein-tyrosyl phosphorylation in T cells from patients with systemic lupus erythematosus: deficient expression of the T cell receptor ζ chain. *J. Clin. Invest. 101:1448.*
16. Brundula, V., L. J. Rivas, A. M. Blasini, M. Paris, S. Salazar, I. L. Stekman, and M. A. Rodriguez. 1999. Diminished levels of T cell receptor ζ chains in peripheral blood T lymphocytes from patients with systemic lupus erythematosus. *Arthritis Rheum. 42:1908.*
17. Pang, M., Y. Setoyama, K. Tsuzaka, K. Yoshimoto, K. Amano, T. Abe, and T. Takeuchi. 2002. Defective expression and tyrosine phosphorylation of the T cell receptor ζ chain in peripheral blood T cells from systemic lupus erythematosus patients. *Clin. Exp. Immunol. 129:160.*
18. Tsuzaka, K., T. Takeuchi, N. Onoda, M. Pang, and T. Abe. 1998. Mutations in T cell receptor ζ chain mRNA of peripheral T cells from systemic lupus erythematosus. *J. Autoimmun. 11:381.*
19. Wu, J., J. C. Edberg, A. W. Gibson, B. Tsao, and R. P. Kimberly. 1999. Single-nucleotide polymorphisms of T cell receptor ζ chain in patients with systemic lupus erythematosus. *Arthritis Rheum. 42:2601.*
20. Nambiar, M. P., E. J. Enyedy, V. G. Warke, S. Krishnan, G. Dennis, G. M. Kammer, and G. C. Tsokos. 2001. Polymorphisms/mutations of TCR ζ chain promoter and 3′ untranslated region and selective expression of TCR ζ chain with an alternatively spliced 3′ untranslated region in patients with systemic lupus erythematosus. *J. Autoimmun. 16:133.*
21. Nambiar, M. P., E. J. Enyedy, V. G. Warke, S. Krishnan, G. Dennis, H. K. Wong, G. M. Kammer, and G. C. Tsokos. 2001. T cell signaling abnormalities in systemic lupus erythematosus are associated with increased mutations/polymorphisms and splice variants of T cell receptor ζ chain messenger RNA. *Arthritis Rheum. 44:1336.*
22. Tsuzaka, K., N. Onoda, K. Yoshimoto, Y. Setoyama, K. Suzuki, M. Pang, T. Abe, and T. Takeuchi. 2002. T-cell receptor ζ mRNA with alternatively spliced 3′ untranslated region is generated predominantly in the peripheral blood T cells of systemic lupus erythematosus patients. *Mod. Rheumatol. 12:167.*
23. Weissman, A. M., M. Baniyash, D. Hou, L. E. Samelson, W. H. Burgess, and R. D. Klausner. 1988. Molecular cloning of the ζ chain of the T cell antigen receptor. *Science 239:1018.*
24. Frank, S. J., B. B. Niklinska, D. G. Orloff, M. Mercep, J. D. Ashwell, and R. D. Klausner. 1990. Structural mutations of the T cell receptor ζ chain and its role in T cell activation. *Science 249:174.*
25. Irving, B. A., and A. Weiss. 1991. The cytoplasmic domain of the T cell receptor ζ chain is sufficient to couple to receptor-associated signal transduction pathways. *Cell 64:891.*
26. Geisler, C., J. Kuhlmann, and B. Rubin. 1989. Assembly, intracellular processing, and expression at the cell surface of the human αβ T cell receptor/CD3 complex: function of the CD3-ζ chain. *J. Immunol. 143:4069.*
27. Romeo, C., M. Amiot, and B. Seed. 1992. Sequence requirements for induction of cytolysis by the T cell antigen/Fc receptor ζ chain. *Cell 68:889.*
28. Letourneur, F., and R. D. Klausner. 1991. T-cell and basophil activation through the cytoplasmic tail of T-cell-receptor ζ family proteins. *Proc. Natl. Acad. Sci. USA 88:8905.*
29. Hall, C. G., J. Sancho, and C. Terhorst. 1993. Reconstitution of T cell receptor ζ-mediated calcium metabolization in nonlymphoid cells. *Science 261:915.*
30. Reth, M. 1989. Antigen receptor tail clue. *Nature 338:383.*
31. Irving, B. A., A. C. Chan, and A. Weiss. 1993. Functional characterization of a signal transducing motif present in the T cell antigen receptor ζ chain. *J. Exp. Med. 177:1093.*
32. Qian, D., I. Griswold Prenner, M. R. Rosner, and F. W. Fitch. 1993. Multiple components of the T cell antigen receptor complex become tyrosine-phosphorylated upon activation. *J. Biol. Chem. 268:4488.*
33. Koyasu, S., A. G. Tse, P. Moingeon, R. E. Hussey, A. Mildonian, J. Hannisian, L. K. Clayton, and E. L. Reinherz. 1994. Delineation of a T-cell activation motif required for binding of protein tyrosine kinases containing tandem SH2 domains. *Proc. Natl. Acad. Sci. USA 91:6693.*
34. Peter, M. E., C. Hall, A. Ruhlmann, J. Sancho, and C. Terhorst. 1992. The T-cell receptor ζ chain contains a GTP/GDP binding site. *EMBO J. 11:933.*
35. Sussman, J. J., J. S. Bonifacino, J. Lippincott-Schwartz, A. M. Weissman, T. Saito, R. D. Klausner, and J. D. Ashwell. 1988. Failure to synthesize the T cell CD3 ζ chain: structure and function of a partial T cell receptor complex. *Cell 52:85.*

36. Tsuzaka, K., I. Fukuhara, Y. Setoyama, K. Yoshimoto, K. Suzuki, T. Abe, and T. Takeuchi. 2003. TCRζ mRNA with an alternatively spliced 3′ untranslated region detected in SLE patients leads to the downregulation of TCRζ and TCR/CD3 complex. *J. Immunol. 171:2496.*
37. Jensen, J. P., D. Hou, M. Ramsburg, A. Taylor, M. Dean, and A. M. Weissman. 1992. Organization of the human T cell receptor ζ/η gene and its genetic linkage to the FcγRII-FcγRIII gene cluster. *J. Immunol. 148:2563.*
38. Gold, D. P., H. Clevers, B. Alarcon, S. Dunlap, J. Novotny, A. F. Williams, and C. Terhorst. 1987. Evolutionary relationship between the T3 chains of the T-cell receptor complex and the immunoglobulin supergene family. *Proc. Natl. Acad. Sci. USA 84:7649.*
39. Exley, M., L. Varticovski, M. Peter, J. Sancho, and C. Terhorst. 1994. Association of phosphatidylinositol 3-kinase with a specific sequence of the T cell receptor ζ chain is dependent on T cell activation. *J. Biol. Chem. 269:15140.*
40. Ravichandran, K. S., U. Lorenz, S. E. Shoelson, and S. J. Burakoff. 1995. Interaction of Shc with Grb2 regulates association of Grb2 with mSOS. *Mol. Cell. Biol. 15:593.*
41. Rozdzial, M. M., B. Malissen, and T. H. Finkel. 1995. Tyrosine phosphorylated T cell receptor ζ chain associates with the actin cytoskeleton upon activation of mature T lymphocytes. *Immunity 3:623.*
42. Bolliger, L., B. Johansson, and E. Palmer. 1997. The short extracellular domain of the T cell receptor ζ chain is involved in assembly and signal transduction. *Mol. Immunol. 34:819.*
43. Weissman, A. M., D. Hou, D. G. Orloff, W. S. Modi, H. Seuanez, S. J. O'Brien, and R. D. Klausner. 1988. Molecular cloning and chromosomal localization of the human T-cell receptor ζ chain: distinction from the molecular CD3 complex. *Proc. Natl. Acad. Sci. USA 85:9709.*
44. Kearse, K. P., J. L. Roberts, and A Singer. 1995. TCR α-CD3 δε association is the initial step in αβ dimer formation in murine T cells and is limiting in immature $CD4^+CD8^+$ thymocytes. *Immunity 2:391.*
45. Kearse, K. P., J. L. Roberts, T. I. Munitz, D. L. Wiest, T. Nakayama, and A. Singer. 1994. Developmental regulation of αβ T cell antigen receptor expression results from differential stability of nascent TCR α proteins within the endoplasmic reticulum of immature and mature T cells. *EMBO J. 13:4504.*
46. Kearse, K. P., J. P. Roberts, D. Wiest., and A. Singer. 1995. Developmental regulation of αβ T cell antigen receptor assembly in immature $CD4^+CD8^-$ thymocytes. *Bioessays 17:1049.*
47. Nambiar, M. P., E. J. Enyedy, C. U. Fisher, S. Krishnan, V. G. Warke, W. R. Gilliland, R. J. Oglesby, and G. C. Tsokos. 2002. Abnormal expression of various molecular forms and distribution of T cell receptor ζ chain in patients with systemic lupus erythematosus. *Arthritis Rheum. 46:163.*
48. Leitner, K. L., M. W. Leimbacher, A. Peterbauer, S. Hofer, C. Heufler, A. Muller, R. Heller, E. R. Werner, B. Thony, and G. Werner-Felmayer. 2003. Low tetrahydrobiopterin biosynthetic capacity of human monocytes is caused by exon skipping in 6-pyruvoyl tetrahydropterin synthase. *Biochem. J. 373:681.*
49. Krummheuer, J., C. Lenz, S. Kammler, A. Scheid, and H. Schaal. Influence of the small leader exons 2 and 3 on human immunodeficiency virus type 1 gene expression. 2001. *Virology 286:276.*
50. Schwarze, U., W. I. Schievink, E. Petty, M. R. Jaff, D. Babovic-Vuksanovic, K. J. Cherry, M. Pepin, and P. H. Byers. 2001. Haploinsufficiency for one COL3A1 allele of type III procollagen results in a phenotype similar to the vascular form of Ehlers-Danlos syndrome, Ehlers-Danlos syndrome type IV. *Am. J. Hum. Genet. 69:989.*
51. Kawamoto, S. 1994. Evidence for an internal regulatory region in a human nonmuscle myosin heavy chain gene. *J. Biol. Chem. 269:15101.*
52. Heath, J. K., J. Southby, S. Fukumoto, L. M. O'Keeffe, T. J. Martin, and M. T. Gillespie. 1995. Epidermal growth factor-stimulated parathyroid hormone-related protein expression involves increased gene transcription and mRNA stability. *Biochem. J. 307:159.*